

**INVESTIGATION OF SURFACE MODIFICATION OF ALUMINIUM  
ALLOY USING B<sub>4</sub>C THROUGH FRICTION STIR PROCESSING**

**A DISSERTATION**

**SUBMITTED IN PARTIAL FULFILLMENT OF THE REQUIREMENTS FOR  
THE AWARD OF THE DEGREE**

**OF**

**MASTER OF TECHNOLOGY**

**IN**

**[PRODUCTION ENGINEERING]**

Submitted by

**[KAPIL DEV PANDEY]**

**(Roll No. 2K17/PIE/06)**

Under the supervision

of

**Prof. QASIM MURTAZA**

**(Professor)**

**Mr. RAVI BUTOLA**

**(Assistant Professor)**



**DEPARTMENT OF MECHANICAL ENGINEERING**

**DELHI TECHNOLOGICAL UNIVERSITY**

**(Formerly Delhi College of Engineering)**

**Bawana Road, Delhi-110042**

## CANDIDATE'S DECLARATION

I, **Kapil Dev Pandey**, 2K17/PIE/06 hereby declare that the major project Dissertation titled **“INVESTIGATION OF SURFACE MODIFICATION OF ALUMINIUM ALLOY USING B<sub>4</sub>C THROUGH FRICTION STIR PROCESSING”** submitted to the department of MECHANICAL, PRODUCTION & INDUSTRIAL ENGINEERING, Delhi Technological university, Delhi in partial fulfillment of the requirement for the award of the **Master of Technology**, in **Production Engineering** was original and not copied from any source without proper citation. This was further to declare that the work embodied in this report has not previously formed the basis for the award of any Degree, Diploma, Fellowship or other similar title or recognition.

Place: Delhi

**Kapil Dev Pandey**

Date:

(2K17/PIE/06)

## **CERTIFICATE**

I hereby certify that the major project entitled “**INVESTIGATION OF SURFACE MODIFICATION OF ALUMINIUM ALLOY USING B<sub>4</sub>C THROUGH FRICTION STIR PROCESSING**”, in partial fulfillment of the requirements for the award of the Degree of **Master of Technology in Production Engineering** and submitted to the Department of Mechanical, Production and Industrial Engineering of Delhi Technological University has been an authentic record work of **Mr. Kapil Dev Pandey (2K17/PIE/06)** carried out under my supervision.

It is to further certify that the matter embodied in this report has not been submitted to any other university or institution by him for the award of any other Degree/Certificate and the declaration made by him is correct to the best of my knowledge and belief.

**Prof. Qasim Murtaza**

Professor

Department of Mechanical Engineering  
Delhi Technological University

**Mr. Ravi Butola**

Assistant Professor

Department of Mechanical Engineering  
Delhi Technological University

**Place:** Delhi

**Date:**

## ACKNOWLEDGMENT

I would like to express my special thanks of gratitude to **Prof. Qasim Murtaza** and **Mr. Ravi Butola** for their guidance, unwavering support and encouragement. This project work could not have attained its present form, both in content and presentation, without his active interest, direction and guidance. His personal care has been the source of great inspiration. He has devoted his invaluable time and took personal care in motivating me whenever I was disheartened.

I would also like to thank Prof. Vipin, HOD (Mechanical Engineering Department), Dr. N. Yuvraj, Prof. Vijay Gautam, Mr. Parvez Ali, Mr. Yashvant Koli for their support and guidance, although they had a very busy schedule in managing the corporate and academic affairs.

I am thankful to the technical staff of Delhi Technological University, Mr Girish Anand, Mr. OM Prakash, Mr. Tek Chand for their support.

My deep and sincere gratitude to my family for their continuous and unparalleled love, help and support. I am grateful to my brothers for always being there for me as a friend and always with me in every situation. I am forever indebted to my parents for giving me the opportunities and experiences that have made me who I am. They selflessly encouraged me to explore new directions in life and seek my own destiny. This journey would not have been possible if not for them, and I dedicate this milestone to them. I cannot forget to take the name of my cousins for helping me to manage the time and managing my journey to complete the project work.

I also want to thank all those who are directly or indirectly support me for my project.

**Kapil Dev Pandey**

**(2K17/PIE/06)**

## TABLE OF CONTENTS

<b>CANDIDATE'S DECLARATION</b>	i
<b>CERTIFICATE</b>	ii
<b>ACKNOWLEDGMENT</b>	iii
<b>TABLE OF CONTENTS</b>	iv
<b>LIST OF TABLES</b>	vii
<b>LIST OF FIGURES</b>	viii
<b>ABBREVIATIONS</b>	xi
<b>ABSTRACT</b>	1
<b>CHAPTER 1: INTRODUCTION</b>	2
1.1 Surface Modification	2
1.2 Requirements	2
1.3 Methods to prepare AMCs	2
1.4 Friction Stir Processing	2
1.4.1 Working Principle of FSP	4
1.4.2 Process Parameters	4
1.4.2.1 Effects of tool speeds	4
1.4.2.2 Effect of multiple passes	5
1.4.3 Advantages of FSP	5
1.4.4 Limitation of FSP	5
1.4.5 Applications of FSP	5
1.4.5.1 Packaging	5
1.4.5.2 Transportation	5
1.4.5.3 Marine Applications	6
1.4.5.4 Building and Architecture	6
1.4.5.5 Foils	6
1.5 Response Surface Methodology	6
1.5.1 Central Composite Design	7
1.6 Matrix Material	7
1.7 Reinforcements	7

1.7.1 Properties of Boron Carbide (B <sub>4</sub> C)	8
1.8 Tool Material Composition and its Properties	8
1.9 Tool Geometry	8
<b>CHAPTER 2: LITERATURE REVIEW</b>	10
2.1 Influence of Input Process Variables on the surface modification using FSP	10
2.2 Research Gap	19
2.3 Research Objective	19
<b>CHAPTER 3: EXPERIMENTAL METHOD</b>	21
3.1 Design of Experiment (DOE)	21
3.1.1 Identification of numerous process control factors	22
3.1.2 Deciding the range of the process factors	22
3.1.3 Developing the design framework	22
3.2 Work piece Composition and its Properties	24
3.3 Processing of Workpiece	24
3.4 Boron Carbide (B <sub>4</sub> C)	25
3.5 Filling of reinforcements in the grooves	26
3.6 FSP Machine Setup	27
3.7 Preparation of samples for Tensile Testing	30
3.8 Preparation of samples for Microstructure and Micro hardness	32
3.8.1 Microstructure Testing	34
3.8.2 Micro Hardness Testing	39
3.9 Recording of responses	40
<b>CHAPTER 4: STATISTICAL ANALYSIS</b>	42
4.1 Introduction	42
4.1.1 Developments of statistical models	42
4.1.2 DESIGN EXPERT Trial Version 11.0.6 Software	42
4.2 Investigating the feasibility of the model	42
4.2.1 Response 1: UTS	42
4.2.2 Response 2: YS	44
4.2.3 Response 3: % Elongation	46
4.2.4 Response 4: Vickers Hardness	48

<b>CHAPTER 5: RESULT ANALYSIS AND DISCUSSION</b>	51
5.1 Analysis of Result	51
5.1.1 Effect of analysis on UTS	51
5.1.2 Effect of analysis on YS	54
5.1.3 Effect of analysis on % Elongation	57
5.1.4 Effect of analysis on Vickers Hardness	60
5.2 Optimization of Result	63
5.3 Point Prediction	64
<b>CHAPTER 6: CONCLUSION AND FUTURE SCOPE OF STUDY</b>	65
6.1 Conclusions	65
6.2 Future Scope of Study	66
<b>REFERENCES</b>	67

## LIST OF TABLES

S.No.	Content	Page No.
Table 1.1	Chemical composition of work piece material	7
Table 1.2	Chemical Composition of H13 Tool Steel	8
Table 3.1	Process control parameters and their breaking points	22
Table 3.2	Design matrix	23
Table 3.3	Chemical composition of work piece material	24
Table 3.4	FSP Machine Full specifications adopted from Advance metal joining lab manual	28
Table 3.5	Optical microscope images at 100x, 200x, 500x and 1000x of the 20 specimens	35
Table 3.6	Recording of responses	40
Table 4.1	ANOVA for Reduced Quadratic model of UTS	43
Table 4.1.1	Fit Statistics of UTS	44
Table 4.2	ANOVA for Reduced Quadratic model of YS	44
Table 4.2.1	Fit Statistics of YS	45
Table 4.3	ANOVA for Reduced Quadratic model of % Elongation	46
Table 4.3.1	Fit Statistics of % Elongation	47
Table 4.4	ANOVA for Reduced Quadratic model of Vickers Hardness	48
Table 4.4.1	Fit Statistics of Vickers Hardness	49
Table 5.1	Predict the mean of Response parameter	64



## LIST OF FIGURES

S.No.	Content	Page No.
Figure 1.1	FSP machine used for the experiment in Advance metal joining lab.	3
Figure 1.2	Schematic diagram of friction stir processing adopted by [13]	4
Figure 1.3	FSP Tool used in experiment	9
Figure 3.1	AA 5083 plate used for the experiment	24
Figure 3.2	Grooves were made with the help of milling cutter	25
Figure 3.3	Grooves without reinforcement on Aluminium 5083 Plate	25
Figure 3.4	Boron Carbide powder used as a reinforcement for the experiment	26
Figure 3.5	Grooves filled with reinforcement of boron carbide nanoparticle	27
Figure 3.6	FSP performed in Advanced Metal Joining Lab	28
Figure 3.7	Capping passes of grooves with probe less tool	29
Figure 3.8	Grooves after the friction stir processing in advance metal joining lab	30

Figure 3.9	Tensile Specimens before testing in UTM machine.	31
Figure 3.10	Tensile Specimens after Testing in UTM machine.	31
Figure 3.11	UTM machine, DTU	32
Figure 3.12	Wet polishing on emery paper	33
Figure 3.13	Wet polishing on alumina powder upon the Cloth	34
Figure 3.17	Vickers Micro hardness Machine Setup	39
Figure 5.1	Graph between Predicted vs Actual points of UTS	51
Figure 5.2	Graph represents the intersection point of UTS	52
Figure 5.3	Contour plot of UTS between TRS and TTS	53
Figure 5.4	3 D response surface graph of UTS between TRS and TTS	54
Figure 5.5	Graph between Predicted vs Actual points of YS	54
Figure 5.6	Graph represents the intersection point of YS	55
Figure 5.7	Contour Plot of YS between TRS and TTS	56
Figure 5.8	3 D response surface graph of YS between TRS and TTS	57
Figure 5.9	Graph between Predicted vs. Actual points of % Elongation	57
Figure 5.10	Graph represents the intersection point of %	58

	Elongation	
Figure 5.11	Contour Plot of % Elongation between TRS and TTS	59
Figure 5.12	3 D response surface graph of % Elongation between TRS and TTS	60
Figure 5.13	Graph between Predicted vs. Actual points of Vickers Hardness	60
Figure 5.14	Graph represents the intersection point of Vickers Hardness	61
Figure 5.15	Contour plot of Vickers Hardness between TRS and TTS	62
Figure 5.16	3 D response surface graph of Vickers Hardness between TRS and TTS	63
Figure 5.17	Optimum Result of Factors	64

## ABBREVIATIONS

ANN	Artificial Neural Network
ANOVA	Analysis of Variance
BLA	Bamboo Leaf Ash
CCD	Central Composite Design
CNC	Computer Numerical Control
C.V.%	% of Covariance
Df	Degree of freedom
EDS	Energy Dispersive Spectrometer
EBSD	Electron Back Scattered Diffraction
FA	Fly Ash
FSP	Friction Stir Process
FSPed	Friction Stir Processed
FSW	Friction Stir Welding
GNP	Graphene Nano Platelets
HYD	Hydraulic
PSN	Particle Simulated Nucleation
RHA	Rice Husk Ash
RSM	Response Surface Methodology
SCC	Stress Corrosion Cracking
SEM	Scanning Electron Microscope
SZ	Stir Zone
TEM	Transmission Electron Microscope
Temp.	Temperature
TRS	Tool Rotational Speed
TSD	Tool Shoulder Diameter
TTS	Tool Traverse Speed
UTS	Ultimate Tensile Strength
XRD	X Ray Diffraction
YS	Yield Strength



## ABSTRACT

Surface modification is the process of enhancing surface properties either through physical, chemical and biological effects in order to achieve superior surface quality. In this dissertation, initially the aluminium composite is prepared using reinforcement of Boron Carbide nanoparticle which is inserted in a groove prepared on the specimen (AA5083 plate). Then, design matrix is generated using central composite design in response surface methodology. Further, the prepared specimens are taken to the FSP machine where experimentation is performed with regard to above designed matrix. Furthermore, the specimens are then taken for various tests including UTS, YS, % Elongation and finally to Vickers Hardness Testing Machine respectively.

Results are noted and taken to ANOVA for checking the feasibility of the designed model. It is discovered that, p values for various responses were less than 0.05 which indicates that model is significant while lack of fit is maintained insignificant. Eventually, for obtaining the optimum values for various responses, F ratio was taken in order to investigate the dominating parameters. Finally conclusion were drawn which reveals that raising the TRS and Number of passes while dropping the TTS promotes better results.

**Keywords:** Ultimate Tensile Strength (UTS), Yield Strength (YS), Analysis of Variance (ANOVA), Tool Rotational speed (TRS), Tool Traverse Speed (TTS) and Friction Stir Process (FSP)

# CHAPTER 1

## INTRODUCTION

### 1.1 Surface Modification

Surface modification is method for amending the surface of the material by including various physical, chemical and biological parameters which are in variation from the original surface found initially. This method is generally adopted to achieve wide range of versatility in surface such as: Roughness, Reactivity, Surface charge and hydrophilicity .

### 1.2 Requirements

Material showing higher strength to weight ratio plays a vital role in various day-to-day application in field of Automobile and Aerospace Engineering where emphasis is laid on higher efficiency and lower fuel consumption [1]. Properties like temperature sustaining capacity, fracture toughness, fatigue bearing capacity and wear resistance are essential in material for fields like automotive, aerospace, defence, marine and recreation [2,6]. For satisfying the demands, material requires a combination of properties for modern infrastructure, equipment and machinery [1, 3]. Characteristic isotropic properties which are found in the Aluminium Metal Composites (AMCs) are usually hard to be present in monolithic material systems [2,4,5]. Aluminium is profoundly known for its superior mechanical, physical and tribological properties in comparison to other base materials [1, 6]. Some of the important features of Aluminium and Magnesium matrix composites are lower density, good wear resistance and corrosion resistance along with high formability with creep which is seen in Automotive, Aerospace and other technology [5, 6].

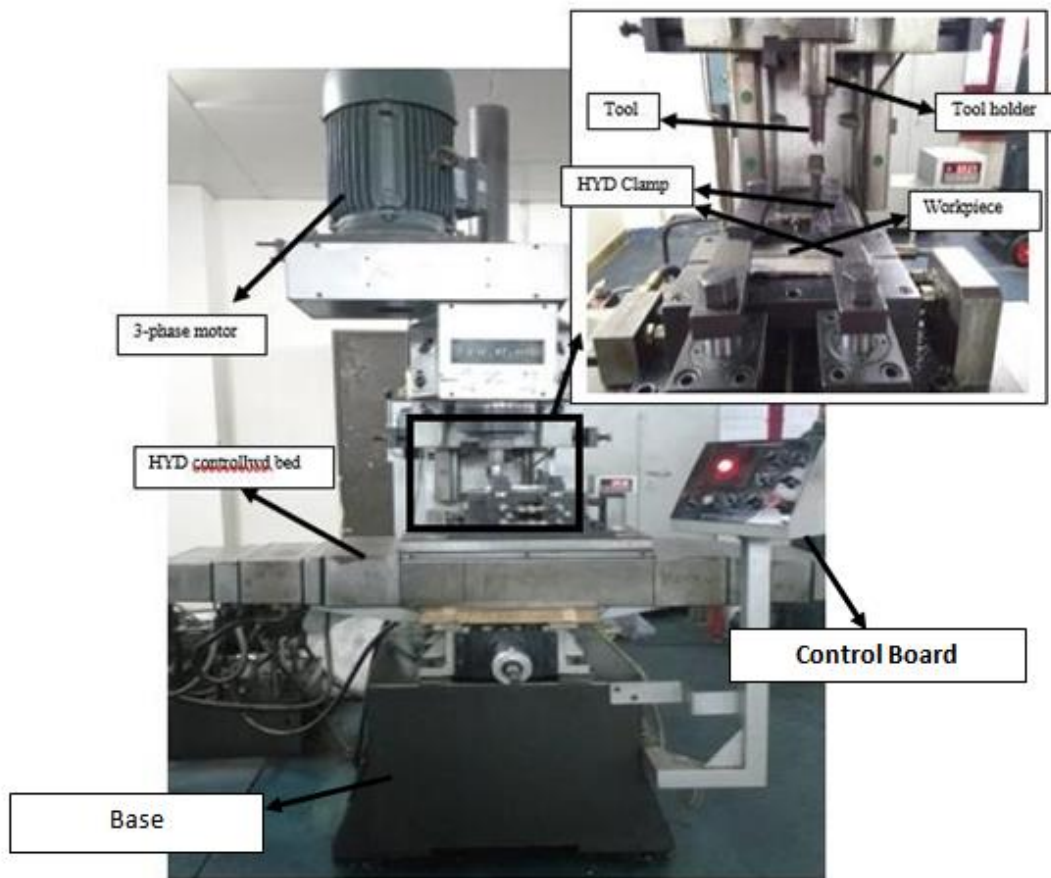
### 1.3 Methods to prepare AMCs

In order to prepare AMCs, there are two methods to prepare it namely Liquid Metallurgy Processing Routes and Solid Route Processing. Sub categorization of the liquid metallurgy processing techniques is done using stir casting, liquid infiltration and various others while solid route processing covers powder metallurgy [1]. Friction Stir processing is the best technique available for the preparation of AMCs, this technique is single step processing which can be referred as solid state processing which is done to achieve micro-structural homogeneity [7].

### 1.4 Friction Stir Processing

Friction Stir processing (FSP) is an extension to Friction Stir welding (FSW) is used for microstructure modification [8]. Significant changes are seen in Microstructures due to the

plastic deformation, mixing and thermal exposure present in the Stir Zone (SZ) [9]. Solid mixing and mechanically activated effect, produced due to extreme deformation of FSP, are the effects manifested while in situ reaction occurs in FSP [8, 10]. Precursor is developed through powder mixture of constituents via conventional hot pressing (HP) or sintering route and after that FSP is performed for fabricating in- situ AMC's [8, 10]. Crucial aim of HP or sintering is to develop billet with sufficient ductility and strength for upcoming FSP. With variations in parameters of HP, variation in in-situ reactions is seen which has a direct impact on microstructure evolution, mechanical properties of composites. This effect is reflected due to size and structure of reinforcing particles developed during sintering [10]. The friction stir process experiment will be conducting at the Figure 1.1 FSP machine used for the experiment in Advance metal joining lab of DTU Delhi with the following experimental set-up.



**Figure 1.1: FSP machine used for the experiment in Advance metal joining lab.**



### 1.4.1 Working Principle of FSP

The tool designed for the processing is non consumable tool, which is developed with two special parts i.e. the bigger shoulder and the smaller lower probe. Initially the tool is given a high rotational speed followed by work piece being brought to contact with tool such that shoulder starts touching the work piece. The tool is provided the motion in such a direction such that plastic deformation and heating supplements the temperature of material and it is deformed with lower flow stress [11]. The combined effect of translation and rotation of the tool generates asymmetry in characteristics at two sides namely the advancing side (AS) where the translation of tool follows the rotation and the other is retreating side (RS) where the direction turns up to be opposite. Figure 1.2 Schematic diagram of friction stir processing adopted by [12] evident that microstructure generated in the two different scenarios will be different. Due to the above processing, Stir zone formation occurs at the centre where due to shear plastic deformation and thermal exposure, at the centre of the processed zone microstructure refinement is absolutely observable.

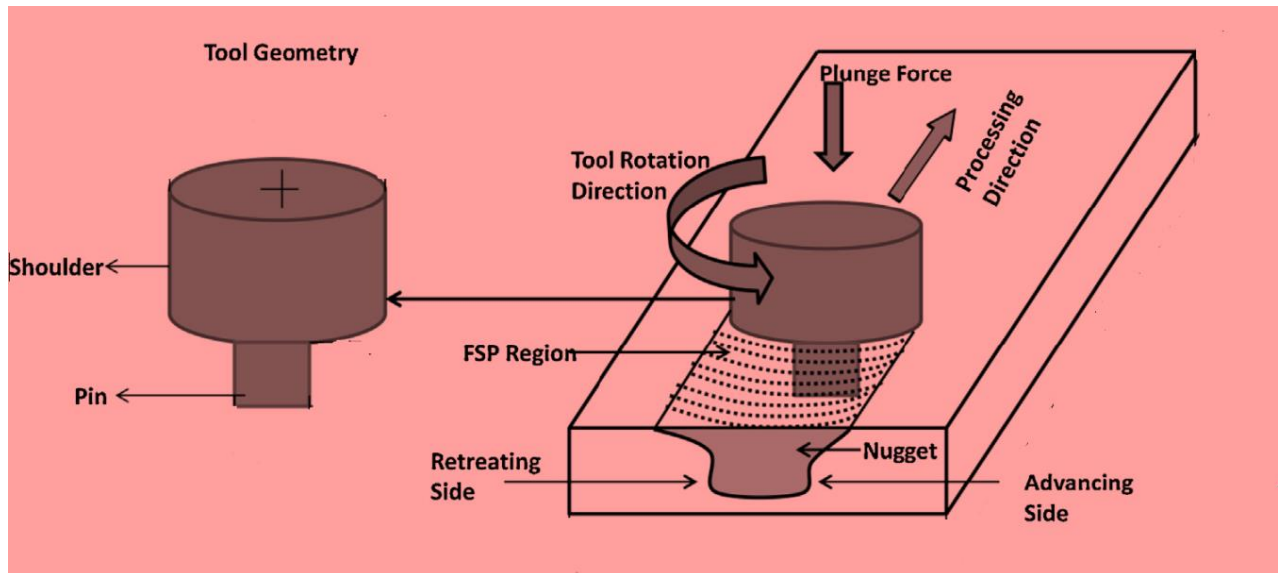


Figure 1.2: Schematic diagram of FSP adopted by [12]

### 1.4.2 Process Parameters

#### 1.4.2.1 Effects of tool speeds

Rotational speed and traverse speed has a direct relationship with heat input which in turn determine the heat input and finally the microstructure and the properties are drawn out. As the heat input is reduced, it increases the grain refinement. [13]

### **1.4.2.2 Effect of multiple passes**

Clustering of reinforcement stands as a crucial matter while developing of composites are concerned. Clustering, although is visible in Nano sized reinforcement. Multi-pass FSP facilitates the decrement in size and structure of cluster maintaining uniformity of reinforcement particles which further diminishes the grain size of matrix [13].

### **1.4.3 Advantages of FSP**

- Processing is either semi-automatic or fully automated as it is based on machine tool technology.
- Rough Surface finish is seen as an outcome of FSP which is useful in reduction of production cost.
- The process is executed quietly.
- Process stands user-friendly because of its automatic nature.
- Process is environmental friendly as well.

### **1.4.4 Limitation of FSP**

- Clamping of workpiece or job stands quite tedious.
- Response action of FSP machines are generally slower than other machines
- Proper intrusion of tool inside the metal is hard to achieve as it requires huge downward forces.

### **1.4.5 Applications of FSP**

Aluminium Alloy has found its applicability in many sectors due to its versatility. For example Food preparation, energy generation, packaging, transportation, electrical transmission and architecture applications. It can be clearly seen that due to the above applicability of Aluminium can serve as an alternative for Steel, Tin plate, Wood, Titanium, Copper, Steel, Zinc, Stainless Steel and many more composites. Descriptive analysis is done in the lower section for more prominence.

#### **1.4.5.1 Packaging**

Aluminium holds the versatility of providing protection from UV light along with corrosion protection and odour contamination during humidity and most essentially its property of being non toxic in nature makes it the most reliable source for packaging purposes.

#### **1.4.5.2 Transportation**

Material Selection for the purpose of transport vehicles such as freight rail cars, ships, buses, boats, coaches, bicycles and in fact the aircraft saw a major flagship with the Aluminium alloys. Strength to weight ratio of Aluminium is the major reason for such a huge contribution of Aluminium in this sector.

#### **1.4.5.3 Marine Applications**

Ship constructions are widely made possible due to availability of aluminium sheets. Aluminium sheds its benefits primarily due to its strength to weight ratio which capacitate it to deliver good performance with available power. Thus some of the parts like surface planning vessels.

#### **1.4.5.4 Building and Architecture**

Industrial flooring and tread plate are the common applicability where the material provides its foil insulation services.

#### **1.4.5.5 Foils**

Aluminium is quite formable which empowers it to be developed as sheets with thickness of 0.2 mm. Foils gets activated through light, gas, oils and fats. Thus foil finds its way in various fields like:-

1. Pharmaceuticals packaging
2. Food protection and packaging
3. Insulation
4. Electrical Shielding
5. Laminates.

### **1.5 Response Surface Methodology**

This optimisation methodology consists of several mathematical and statistical techniques which facilitates analysis of problem where the responses or outputs are dependent on various input variables and the purpose is to optimise the responses. RSM is extensively used at positions where the input variables are having a direct dependency on the responses which determines the quality characteristics of the product. RSM generally includes more than 1 input variable which is in approach of the scientist or the experimenter. RSM tries to develop a relationship between the variables and the responses by initiating a low order polynomial. For example

A first-order model with 2 independent variables can be expressed as

$$Y = b_0 + b_1x_1 + b_2x_2 + e \quad (1.1)$$

If there is a curvature in the response surface, then a higher degree polynomial should be used. The approximating function with 2 variables is called a second-order model:

$$Y = b_0 + b_1 + b_2 + b_{11}.x^2_{11} + b_{22}.x^2_{22} + b_{12}.x_{12} + e \quad (1.2)$$

Method of Least square is used for best approximation of the polynomial relation between response and variable. Collection of data in an organised format helps to determine the polynomial relationship in the most accurate form [14].

### 1.5.1 Central Composite Design

A Central Composite Design normally called 'a focal composite configuration,' contains an imbedded factorial or fragmentary factorial outline with focus focuses that is enlarged with a gathering of 'star focuses' that permit estimation of arch. In the event that the separation from the focal point of the outline space to a factorial point is  $\pm 1$  unit for each factor, the separation from the focal point of the plan space to a star point is  $\pm\alpha$  with  $|\alpha| > 1$ . The exact estimation of  $\alpha$  relies upon specific properties wanted for the plan and on the quantity of components included. Also, the quantity of focus point runs the plan is to contain additionally relies upon specific properties required for the plan [14].

### 1.6 Matrix Material

Aluminum alloy 5083 is used for fabricating vehicle bodies, mine skip cages, tip truck bodies etc. AA5083 work pieces of dimension 200mm x 80mm x 6mm and composition as given in Table 1.1 used in this study [15].

**Table 1.1: Chemical composition of work piece material [15]**

Element	Mg	Si	Mn	Cr	Fe	Cu	Zn	Ti	Al
Comp. (%)	4.5	0.2	0.7	0.09	0.7	0.26	0.04	0.05	Balance

This aluminium alloy is produced in many tempers such as 5083-O, 5083-H111, 5083-H32 and 5083-H131. Aluminium 5083 has low density and high strength, thus the resulting high strength to density ratio makes it common among applications such as transport, marine, automotive, aviation and defence.

### 1.7 Reinforcements

Reinforcement is generally produced through agro waste and industrial material in which the most common ones are red mud, FA, BLA, bagasse ash and RHA [1,16,17,18]. Low density and

low thermal coefficient of expansion are the crucial characteristics of composites. For the investigation purpose, B<sub>4</sub>C is selected as the nano particle for development of composite and eventually its effectiveness on the mechanical properties is put to focus.

### 1.7.1 Properties of Boron Carbide (B<sub>4</sub>C)

Boron Carbide being one of the best ceramic materials possess properties such as low density, extremely good hardness, good chemical stability and neutron absorptive capability. Other special quality of this reinforcement ionizing radiation, toughness stands close to diamond. Sintering aids needs to be supplemented for sintering at high relative densities. It also possesses good nuclear properties. With evidence to the above properties, this ceramic material is chosen for experimentation purpose, with size specification of 60 nm [19]

### 1.8 Tool Material Composition and its Properties

H13 Tool Steel was bought from Anand Parbat Industrial Area and is used for the experiment. Its composition and properties are as discussed below in the Table 1.2.

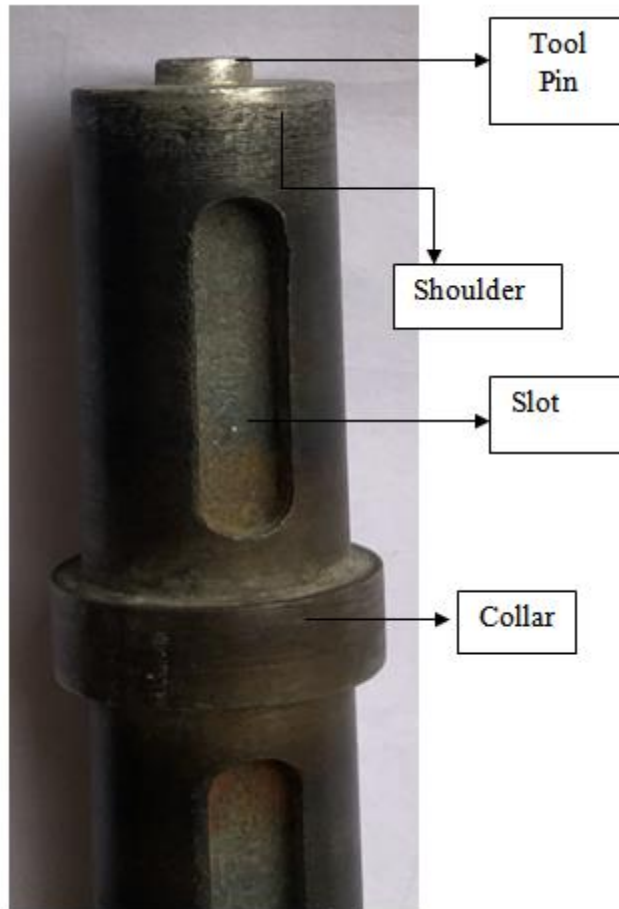
**Table 1.2: Chemical Composition of H13 Tool Steel [20]**

Element	C	Mn	Si	Cr	Mo	V	Fe
%	0.40	0.40	1.00	5.25	1.35	1.00	Balance

**H13 Tool Steel** is a hot worked chromium-molybdenum steel that is prominently used in hot work as well as cold work tooling applications. The hot hardness of this tool steel resists thermal fatigue cracking which occurs due to the repeated cycles of heating and cooling while performing hot working. Because of its excellent combination of high toughness and resistance to thermal fatigue cracking H13 is prominently used for more hot work tooling applications compared to other tool steel. H13 tool steel has high toughness and good stability in heat treatment therefore it is also used in a variety of cold work tooling applications. In these applications, H13 also provides better wear resistance and harden ability as compared to common alloy steels [20].

### 1.9 Tool Geometry

The collar diameter has taken as 29.4mm, the collar thickness has taken as 10mm, the shoulder diameter has 19.95mm, and the probe diameter has 7mm. The Figure 1.3 is shown following below:



**Figure 1.3: FSP Tool used in experiment**

## CHAPTER 2

### LITERATURE REVIEW

#### 2.1 Influence of Input Process Variables on the surface modification using FSP

The Literature Review of the project in the form of Paragraph consists of the selection of the material of work piece and different research work added in the area of interest of topic of this project.

R. Vaira et al. [15] applied the FSP on AA5083 with the agenda of enhancing the wear resistance. FSP was conducted using face centred central composite with initial input parameters as TRS, TTS and TSD. Results were carried out which depicts that the wear resistance of most of the FSPed specimens were greater than initial material and eventually a model is prepared to analyse the correlation between the process parameters and the wear resistance.

Vipin et al. [21] worked on Aluminium alloy by considering speed, feed and depth of cut as the initial input parameters for the purpose of performing FSP. Optimisation is carried using Taguchi orthogonal array with its 3 levels. The entire experimentation is delivered through CNC with specifically designed tools.

Nitin et al. [22] worked on AA7005 alloy for purpose of enhancing resistance using titanium and boron carbide reinforcement nanoparticles. Surface composites were prepared using FSP which was further tested using the Micro Hardness Test and depth of penetration. Results manifested that both micro hardness and depth of penetration were higher than the initial base metal, thus ballistic mass efficiency got improved significantly.

Ali et al. [23] worked on Aluminium composite having SiC nanoparticles. The developed specimens were tested to check various properties such hardness, ductility, yield strength and finally the tensile properties. Significant improvements were registered in terms of hardness, while strain rates saw a hike at elevated temp. Finally it can be stated that YS was also improved tremendously up to 240% as seen by the data obtained through results.

Issac et al. [24] worked on Aluminium AA6061 along with some components of Magnesium and Cu, where the reinforcement used is FA, which is cost effective by nature. After the successful preparation of composition it is put to various equipments namely optical microscope, SEM and finally EBSD.

Z.Y. et al. [25] worked on Aluminium 6061 grade where reinforcement particles like  $ZrB_2$  are consumed. The objective of study is to investigate impact of  $ZrB_2$  addition on the

Microstructural and Tensile properties. Once the experiment was executed results were drawn out which reveals that Addition of  $ZrB_2$  responded in regular decrement in grain size due to the intentional pressing of the boundary migration and/or orientation. Similarly presence of refined grains and  $ZrB_2$  nano dispersions also led to valuable improvement in micro hardness, strength and hardness of the FSPed composite in contrast with the processed 6061 Al Alloy.

Liyang et al. [26] focused on the impact of the grain structure on the SCC of the FSP AZ80 Mg alloy and simultaneously examined various properties like static, electrochemical and SCC, microstructural study and physical properties. Test were conducted for various sized particle i.e both fine and coarser ones. While performing slow strain rate tensile test it was observed that FG specimens come up with anisotropy with SCC susceptibility in both the directions. Pitting corrosion formation was drastically increased whereas SCC performance was seen declining due to the texture softening effect.

Naresh et al. [27] worked on Aluminium and Magnesium combined alloy (AA5086) by processing it using FSP with different passes and thereby understanding micro structural development. Through weakening crystallographic texture development was impacted as strain induced circumference movement was the influential parameter of microstructure development in the alloy. There was variation in the crystallographic texture as shown by the micro texture measurements along the thickness of the sample.

Guoqiang et al. [28] worked on Aluminium Copper based system i.e Al 1060 variant. The specimen is processed on FSP machine where the impact of the number of passes, microstructure and wear behaviour were studied. While raising the number of passes it was noted that only  $Al_2Cu$  phase formation took place. The specimens were taken to SEM and TEM for the purpose of results generation which demonstrated that two types particles were generated namely the finer and coarser Cu- $Al_2Cu$ , which is further converted to  $Al_2Cu$  particles. Care should be taken while performing FSP in opposite direction in relation with the consecutive pass, as it will be responsible for reducing the size of the particles.

S. S. Nene et al. [29] worked on AX-M541 and prevailing AXM series Mg alloy simultaneously to check and evaluate microstructural refinement and other physical properties on an examination basis. Uniform dispersion is seen throughout the microstructure for the FSP led Al-Ca (C36) with severe refinement. PSN is an observed phenomenon which occurs for a specific sized particle due to heating effects after performing FSP. Dispersion Strengthening can be seen



as the major key role for raising the strength. AXM541 demonstrated superior mechanical qualities over pre existing AXM alloys due to improved refining of Al-Ca phase obtained from FSP.

Qu Liu et al. [30] worked on cast AZ91 magnesium alloy using FSP. Results manifested that the corrosion rates are significantly lowered as per electrochemical and hydrogen evolution measurements. This result implies directly to the variation of corrosion process a raised due to the amendments in the texture and uniform contribution of particle during FSP. Enhancement of reliability and accuracy of the corrosion product film occurs due to the creation of thin and regular beta phase layer on FSP layered surface due to the rigid fine beta phase formation formed.

Marek et al. [31] found that surfacing, spraying or re-melting are basically the usual methods utilized in the formation of surface layers with the help of laser beams. Thus a newer method commonly referred as FSP is used primarily for the enhancement of microstructure in near surface layers of working intermetallic parts. This process is responsible for generating small grained structures, for developing alloy with certain elements and enhancement of welded joints qualities. This study was categorised into several section where the advantages of the FSP is discussed. Then the study is focussed on the analysis part further it is laid on the microstructure refinement process and finally the investigation go about FSP with ultrasonic vibration.

G.K. et al. [32] classified the friction stir technologies into two major categories i.e primarily welding is discussed while the other department shares concern for FSP technologies. This study is fully focussed with dealing the improved and improving FSP technologies along with its various input parameters, achieved properties of their products and its adequacy and versatility to various metals.

Devinder et al. [33] suggested the processing of solid solution can be done through FSP using mechanical alloying tool. Zinc was introduced in Aluminium while performing multi variable FSP which resulted in solubility and further highly saturated solid solution is generated. Experimentation testing is processed using XRD and SEM. It is seen that hardness was significantly improved in the stirred areas because of the presence of Zn, in comparison to the base metal. Surprisingly, the Zn introduced in the initial pass gets decomposed in the next pass along with the precipitation formation takes place. Further, thermal reliability of the

microstructure got enhanced in conjecture to the abnormal grain growth after the first pass. Peculiarly it is rather noticed that equal sized particles are generated in the process of FSP.

Z.W. et al. [34] worked on graphene nanoplatelets composites which are developed by joint collaboration of powder metallurgy and FSP. Results manifested that GNP distribution got enhanced by raising the Number of Passes in FSP. It is evident that layered GNP's are well structured. Finally it is observed that through tensile test that % elongation delivers a hike initially and then a drop is seen as the number of passes in FSP is raised.

Sudhakar. M et al. [35] researched on numerous matrix materials with reinforcements. Microstructure was keenly observed using SEM while micro-hardness was encountered using Vickers Hardness testing technique, similarly TRS and TTS were also emphasised. Surface composites which are effectively developed by the practical application of FSP is studied and important suggestion to new researchers are also provided.

Anshul et al. [36] worked on two grades of Mg and one on the steel grades by emphasising FSP on the specimens. Primarily the study was focussed to gain insights of mechanical properties such as hardness, tensile strength etc. The major observation that become evident are that the FSP lead to refinement of grain size into finer magnitude, thus grain growth is seen. Experimentation was carried at variable speeds and angles with FSP tool which resulted in variation of properties in the FSP.

Saurabh et al. [37] worked on aluminium alloy by processing it through artificial intelligence tool and then passing it for FSW. L27 orthogonal array is followed for performing the experimentation. Further experimentation is processed using ANN which is basically a model for generating results for tensile strength, micro hardness etc using L27 matrix. Hybrid approach concerning the collaboration of ANN and genetic algorithm is applied. Results showed significant improved and finally conclusions were drawn.

G. Hussain et al. [38] worked on Al 7075 alloy for the analysis of neural network. Experimentation involved analysing the effect of feed rate and spindle speed on % elongation, tensile strength and on electrical energy.

S. Soleymani et al [39] considered studying about Aluminium composites having reinforcement of SiC and MoS<sub>2</sub> particles for performing FSP operation which is wear resistant in nature. Several experiments are carried out regarding the tests such as wear behaviour, hardness etc. Eventually the two variants are examined for evaluation. Hybrid composite delivered similar

contribution of reinforcement in the insertion zone and tremendous attachment is observed between the processing layer and the basic metal. Wear resistance is also significant in case of hybrid composites. Further research indicated that while dominant wear mechanism were studied in sliding conditions of samples, light hampering was evident along with wear of hybrid composite is also seen.

Thangarasu et al. [40] developed the specimens using AA6082/TiC and to investigate the effects of adding TiC and the impact of adding variable quantities i.e. volume fractions on Microstructure along with dry sliding wear behavior. The specimen were basically operated at a speed of 1200 rpm with a TTS of 60mm/min and plunger force of 5KN. SEM was used for the experimentation purposes. Results generated manifested that rate of wear dropped significantly as the volume fraction of particles increased.

P.R. et al. [12] worked on Al-Si alloy which is developed through FSP at variable speed ranging from 800rpm to 1400rpm and its speed vary from (60-150)mm/min and the plunger force developed between (4-9)KN. Experimentation was carried out using SEM and optical microscope. Results were generated to study the changes in mechanical properties and machinability of the specimen. Finally it was registered that YS, UTS and ductility got increased significantly.

A.G.et al. [41] worked on hypereutectic Al-30Si alloy through FSP in order to enhance the machinability and thus trying to establish good tool life for machining operations. The specimens that were encountered are handled at 900 rpm speed, TTS of 16 mm/min. SEM was exclusively used for the experimentation purposes. Poor machinability is seen with surface roughness of FSPed surface being improved over the conventional.

M.A. et al. [42] worked on Al-Mg alloys in order to analyse its super plastic behavior and determine the microstructure. The specimen with dimensions of 16 mm diameter is chosen and it is processed with 400rpm and a TTS of 0.42 mm/sec through FSP. Experimentation is followed by using SEM and optical electron microscope respectively. Results manifested that stability is maintained at high temperature for microstructure imaging, secondly huge heat concentration is seen during FSP and finally good super plastic behavior is seen.

Sandeep et al. [43] worked on Al-Si hypoeutectic A356 alloy to check the wear behavior and machinability thus improving its wear resistance and machinability by multiple passing it through FSP. The specimen works at 800 rpm with a TTS of 120mm/min and plunger force

9KN. The experimentation is carried out with optical microscope and pin-on disc method using a tribometer. Results came up with conclusion that wear resistance was improved with lower coefficient of friction and further the ductility seemed more developed.

Sumit et al. [44] investigated hypoeutectic Al-Si alloy for the purpose of grain refining and checking the mechanical behavior. Experimentation was carried out with specimen dimensions of 5 mm pin diameter and with input parameters of 800 rpm and with TTS of 120 mm/min and having a plunger force of 9KN. Instruments implemented for the experimentation purpose were SEM for the microstructure identification whereas for the hardness purposes Vickers micro hardness is implemented and finally strength is tested through Tensile testing. Results manifested that average hardness and ductility significantly improved as the number of passes were raised.

S. Joyson et al.[45] worked on generation of aluminum matrix composites having quartz particulate reinforcement SiO<sub>2</sub> particles. The tool used for the process is HCHCr with the input parameters being 1600 rpm and TTS of 60mm/min and a plunger force being fixed at 10 KN. The equipment used for the process are optical scanning and TEM. Results shows that quartz particles were uniformly distributed in the SZ and by virtue of high strain rate deviation of shape and size is encountered.

I Dinaharan et al. [46] worked on AA6082 aluminium matrix composites with various ceramics particles such as SiC, Al<sub>2</sub>O<sub>3</sub>, TiC, B<sub>4</sub>C and WC using HCHCr at TTS of 40mm/min and 1000 rpm of TRS. The instrument used for the analysis is SEM. Results gathered out of the experiment were that area of the SZ was influenced by speed, TTS and with the groove width. Micro hardness and wear rate is affected significantly.

Issac et al. [47] analyzed copper matrix composite (CMC's) which are produced using FSP that are worked at 1000 rpm with a TTS of 40 mm/min and plunger force of 10KN. Experimentation was carried out using SEM. Finally the results presented that SZ, grain size, micro hardness and wear rate got a slight variation only.

G. V.V. et al. [48] selected AZ91 Mg alloy with its specimen dimensions having pin diameter of 3mm with 1mm taper diameter with a TRS of 1400 rpm, TTS of 25 mm/min, TSD of 15mm. The experimentation was performed using optical microscope and by using XRD, Vickers indentation method was adopted for micro hardness purposes. Results gathered manifested that grain refinement was significant and hardness was lowered after the FSP .Secondly due to the grain refinement and solid strength solutioning cutting force saw a slight hike.

N. Yuvraj et al. [49] adopted fusion and solid state processing for the purpose of preparing aluminium composites by incorporating nanoparticles of Boron carbide in Aluminium 5083 using Tungstun Inert Gas (TIG) arc process and FSP. The specimen chosen were provided with TRS of 1070 rpm, TTS of 40mm/min and a plunger force of 40 KN. Experimentation was carried out by SEM, Field emission gun SEM and an EDS was used. Results manifested that the thickness achieved is greater in comparison to the TIG method, similarly greater hardness and wear resistance is seen with TIG based specimen but the micro hardness drops in case of TIG arc based specimen but the wear resistance of the specimen with TIG based is lowered in comparison to FSPed specimen.

Marek Stanislaw et al. [50] worked on FSP in which the monolithic elements microstructure is enhanced. FSP can be dedicated towards surface spraying by using laser beam. For developing fine microstructure, certain parameters such as TRS, TTS and TA can be manipulated. FSP is a precise working machine which stands acceptable for alloying surfaces and welded joints.

H.R. Lashgari et al. [51] emphasised on the impact of variation of various elements such as Co, Cr, Mo along with including FSP on Microstructure in its different states. Scanning electron microscopy was deployed for analysing two different states namely as-cast and solutionized states. Other techniques which were implanted in action were EBSD and XRD technique for crystal structure identification

Vijay Kurt et al. [52] extend its focus on surface roughness and micro-hardness of Aluminium alloy. Primarily the optimisation is carried forward with RSM using the central composite design where the input parameters chosen are surface roughness and micro-hardness, finally regression equation is developed which is quadratic in nature. ANOVA is taken into consideration for the feasibility of the model working.

Honglog Zhao et al. [53] worked on Aluminium 6061 alloy by processing FSP wherein similar equiaxed Al grains are formed in weld zone. Observations reveal that as the speed of operation is raised the size of grains starts to rise. In terms of comparative analysis, the upper half gets to see larger grain size than the lower half. Similarly when the numbers of passes were raised the size variation was quite evident. At higher rotational speed of about 700 rpm weld nugget and thermo mechanically affected heat zone (TMAZ). Eventually, strength analysis manifested that at lower speeds the base material performed well in comparison with specimen adopted with FSP but as the speed is increased the FSP adopted specimen showed higher strengths

R.S. Mishra et al. [54] used Al alloy for performing FSP. The various parameters chosen for the process are speed, movement of tool, depth and the tilt angle. Temperature ranges of upto 500° C can be achieved. Basically there are 3 regions where the presence of FSP is evident namely the heat affected zone, nugget zone and finally the thermo mechanically affected heat zone. Various factors such as tool geometry, cylindrical pins are responsible for sound welds.

M. Sharifitabar et al. [55] emphasis its investigation on composites related to Aluminium produced by adopting FSP. Primary focus is to visualize the mechanical properties and microstructure wherein error free surface is to be developed by high speed and tilt angle of pin. By convention it is seen that as the number of passes are raised, fine regulation in scattering of nano particle will be observed. Similarly, passes increment often bring about reduction in grain size followed by tensile and yield strength being raised significantly. Similarly, elongation is also being propagated.

G. M. Karthik et al. [56] considered magnesium alloy for the investigation purpose by processing it using FSP. The FSP being adopted includes two passes with variation of rotational speeds. Tests such as micro tensile testing and microstructure are performed. Microstructures imaging is done using the scanning electron microscope which is further magnified using the dynamic crystallisation mechanism. Finally the author preferred to perform the grain refining and texture generation of Mg-Al-Zn.

Stephen et al. [57] worked on AlSi10Mg parts through FSP which is simultaneously passed on for selective laser melting for improvement in properties which is observed using the Microstructures. Various results were plotted which manifested that as built models were better in cases of hardness and microstructure in comparison to HIPed, whereas for the HIPed residual stresses were relatively lower than as-built. Finally a graphical representation is developed to judge the hardness of AlSi10Mg part which can further be used for FSP selection.

Felice Rubino et al. [58] tried focusing on Ti-6Al-4V FSPed plates which is prepared using electron beam melting by using ARCAM A2X machinery. Focus is also laid on calculation of morphology and measuring microhardness. Results manifested that if traverse speed is maintained high, surface quality might suffer along with there is incremental hardness observed in latter cases.

Masoud Roknain et al. [59] worked on Cu-TiO<sub>2</sub> composites which is prepared using FSP , further optical microscopy and field emission SEM is used for microstructural studies and finally

tensile testing is carried. Results manifested that there was significant decrement in grain size while remarkable increment is seen in tribology sector as the Number of passes were regulated to bigger numbers due to FSP. Finally the author discussed the amendments seen in corrosion behaviour.

Bing Zhang et al. [60] worked on AE42 alloy which contains Magnesium in it. Various processes are carried out such FSP on milling machine which is further worked on optical microscopy, XRD, SEM and finally to Electron Backscattered diffraction. Results manifested shortening of grains and homogeneity of microstructure is observed as well due to aging treatment. Other parameter which saw a hike is yield strength and the ultimate tensile strength.

Yifu Shen et al. [61] worked on SiC/Al composite through FSP which is further studied using the optical microscopy and then microhardness test is being performed along with dry sliding wear test is focussed. The author aimed to conduct this test in order to investigate the mechanical properties and to check the microstructure. Results manifested that composites prepared by FSP occupies higher hardness having one tool further, it is observed that friction coefficient is lowered in the above cases. A switch of mechanism is observed from adhesive to abrasive due to lower size of SiC.

Behnam Lotfi et al. [62] worked on Al-Al<sub>3</sub>Ni/TiC composite through FSP using Reactive Powder which is prepared using alloying elements Ni, Ti and C powder for 20 hrs thereby generating Al-Al<sub>3</sub>Ni particles. Higher temperatures and hardness can be achieved by performing higher number of passes in FSP

M. Sarkari et al. [63] investigated a special type of FSP which includes cryogenic in it due to which an abnormal grain growth is seen. Experimentation is carried forward using SEM and electron backscattering detector. Observation detected that unusual growth in particles due to low temperature.

Yefeng Bao et al. [64] worked on FSPed AZ31B Mg alloy which is prepared by FSP and then the microstructure and mechanical properties is focused wherein the equipment used are TEM and EBSD. Finally the tensile test is performed and the yield strength values and elongation is taken into consideration by various forming methods. The adopted grain refinement technique is dynamic crystallisation method.

Jinu Paul et al. [65] worked on composites of graphene along with Al6061 by performing FSP. Experimentation is carried out using Optical Microscopy. The author wish to evaluate the

material using MMCRF and SCRF tests. Results manifested that as we proceed from SCRF to MMCRF mechanism, it will be observed that the width of processing zone is developed similarly the grain refinement is improved. The author concluded that material's surface hardness and UTS is profoundly raised in MMCRF in comparison to SCRF.

Y. F. Yen et al. [66] worked on Fine grained Aluminium Matrix composites wherein the additions added included that of shape memory alloy for the purpose of FSP. It is observed that the mentioned shape gets well diffused in the Aluminium Matrix; it is also observed that no extra bindings are found at the interfaces of well bounded areas. Further detailed investigation also projected that with supplementation of Ti and Ni particles the dynamic recrystallization can be improvised due to particle stimulated nucleation.

Qasim et al. [67] developed spherical powders having a diameter size of 50  $\mu\text{m}$  for the purpose of performing Sintering. Author wishes to construct ball milled Aluminium alloy. Experimentation is carried out using XRD, SEM and EDS. Results manifested the impact of milling in order to investigate the parameters of alloy powder.

## **2.2 Research Gap**

On the basis of the literature survey, following research gap can be extracted:-

- Very few studies related to coating in the surface of aluminium alloy AA5083 of FSP zone are mentioned in literature.
- Various types of reinforcement (Artificial and different type of natural reinforcement) can be used during modification of surface of aluminium alloy AA5083 with the help of FSP to enhance the micro structural and physical properties.
- Refrigeration of FSP zone is mentioned in very rare literatures. Cooling Agents which can be employed for such purpose could be water, liquid nitrogen and methanol respectively.
- Ballistic resistive capacity and fatigue resisting nature of composites are mentioned rarely in literatures

## **2.3 Research Objective**

On the basis of the literature survey, following research objectives can be extracted:-

- To enhance the mechanical properties by the modifying the surface of metal using FSP
- To prepare the samples of Aluminium with dimensions 200×80×6 mm.
- To prepare the solution of layer of B4C reinforcement.



- To study the effects of various parameters such as TRS, TTS, Number of passes using RSM.
- To study the microstructure of the samples with the use of optical microscope.
- To study the effect on UTS, YS, % Elongation and Vickers Hardness.

## CHAPTER 3

### EXPERIMENTAL METHOD

#### 3.1 Design of Experiment (DOE)

In the detailed research studies, it is quite evident that FSP process parameters such as depth of penetration, traverse speed, tool tilt angle etc has a crucial role to play in physical and chemical properties of the applied specimen. Traditional design technique is applied in areas where a single parameter is varied and its impact is visualised, which implies a requirement to perform several experiment in order to investigate its significance. The entire process is quite tedious and time killing.

Basically the experiment design processes consist of 3 fundamentals:

**Randomization:** - Experimental runs should be arranged in a random order for the purpose of neutralizing the impact of outer noise factors.

**Replication:** - For every factor combination it is anticipated to achieve similar experimental runs which helps in calculation of experimental errors generated. For identifying if given differences in the data are mathematically varying; error measurement is the crucial element.

**Blocking:** - This parameter is helpful in mitigating the impact of factors which influences the response but is quite insignificant for our purpose. These are referred to as noise factors. Similar experimental situations are generally referred to as Block, in which the experimenter partitions up the investigation from the mathematical design into groups that follows each block [14].

Entire process is carried forward for investigating the input parameters and to develop statistical models to understand the connection among the parameters.

Steps followed to achieve the above condition are:

1. Identification of essential process control factors
2. Deciding the working scope of the procedure control factors, viz. TRS, TTS and Number of Passes
3. Developing the design matrix
4. Conducting the examinations according to the design matrix
5. Recording the reactions viz. Vickers hardness, % Elongation, UTS and YS.
6. Developing the numerical models
7. Checking the adequacy of the models
8. Finding the significance of coefficient
9. Developing the final proposed models

10. Plotting of diagrams and drawing conclusion
11. Discussion of the outcomes

### 3.1.1 Identification of numerous process control factors

On behalf of the FSP geometry there are basically 3 specific parameters which need to be considered such as the TRS, TTS and number of passes. For the experimentation purpose the considered parameters are Vickers hardness, % Elongation, UTS and YS.

### 3.1.2 Deciding the range of the process factors

Preliminary runs are performed by varying a single parameter while maintaining the other parameters as constant. Working range is kept constant by observing the FSP geometry for the smooth appearance and the Non-appearance of fixed deformities.

The upper and lower limits were coded as +1 and -1, individually. The coded esteems for middle of the road esteems can be computed from the relationship, Where,  $X_i$  is the required coded estimation of a variable X, when X is any estimation of the variable from  $X_{min}$  to  $X_{max}$ ;  $X_{max}$  and  $X_{min}$  are the most extreme and least levels of the factors. They chose procedure parameters and their upper and lower restrains together with documentations and units are given in Table 3.1.

**Table 3.1: Process control parameters and their breaking points**

S.NO.	Parameters	Units	Notations	-1	0	+1
1.	Tool Rotational Speed	RPM	TRS	700	1000	1300
2.	Tool Traverse Speed	mm/min	TTS	30	45	60
3.	Number of Passes	unit	unit	1	2	3

### 3.1.3 Developing the design framework

A 3 factor 3 level composite design matrix was utilized for the experiment. A Face centered CCD matrix covers more noteworthy design space than the factorial design matrix lattice,

consequently bringing about more prominent exactness of the established relationship [43].

Table 3.2 demonstrates the 20 sets of coded conditions used to frame the outline lattice-

**Table 3.2: Design matrix**

Std	Run	Coded value of TRS	Coded value of TTS	Coded value of Number of Passes	Actual value of TRS (RPM)	Actual value of TTS (mm/min)	Actual value of Number of Passes (unit)
1	9	-1	-1	-1	700	30	1
2	20	1	-1	-1	1300	30	1
3	17	-1	1	-1	700	60	1
4	12	1	1	-1	1300	60	1
5	8	-1	-1	1	700	30	3
6	7	1	-1	1	1300	30	3
7	15	-1	1	1	700	60	3
8	1	1	1	1	1300	60	3
9	11	-1	0	0	700	45	2
10	19	1	0	0	1300	45	2
11	5	0	-1	0	1000	30	2
12	2	0	1	0	1000	60	2
13	3	0	0	-1	1000	45	1
14	18	0	0	1	1000	45	3
15	14	0	0	0	1000	45	2
16	16	0	0	0	1000	45	2
17	6	0	0	0	1000	45	2
18	10	0	0	0	1000	45	2
19	4	0	0	0	1000	45	2
20	13	0	0	0	1000	45	2

### 3.2 Work piece Composition and its Properties

AA 5083 is used for the experiment. The size of workpiece used is 200mm (length), 80mm (width) and 6mm (thickness) as per the requirements of Friction Stir Processing Machine present in Delhi Technological University. A total of 10 plates were used to perform 20 experiments. The composition of AA5083 is as follows in Table 3.3:

**Table 3.3: Chemical composition of work piece material [15]**

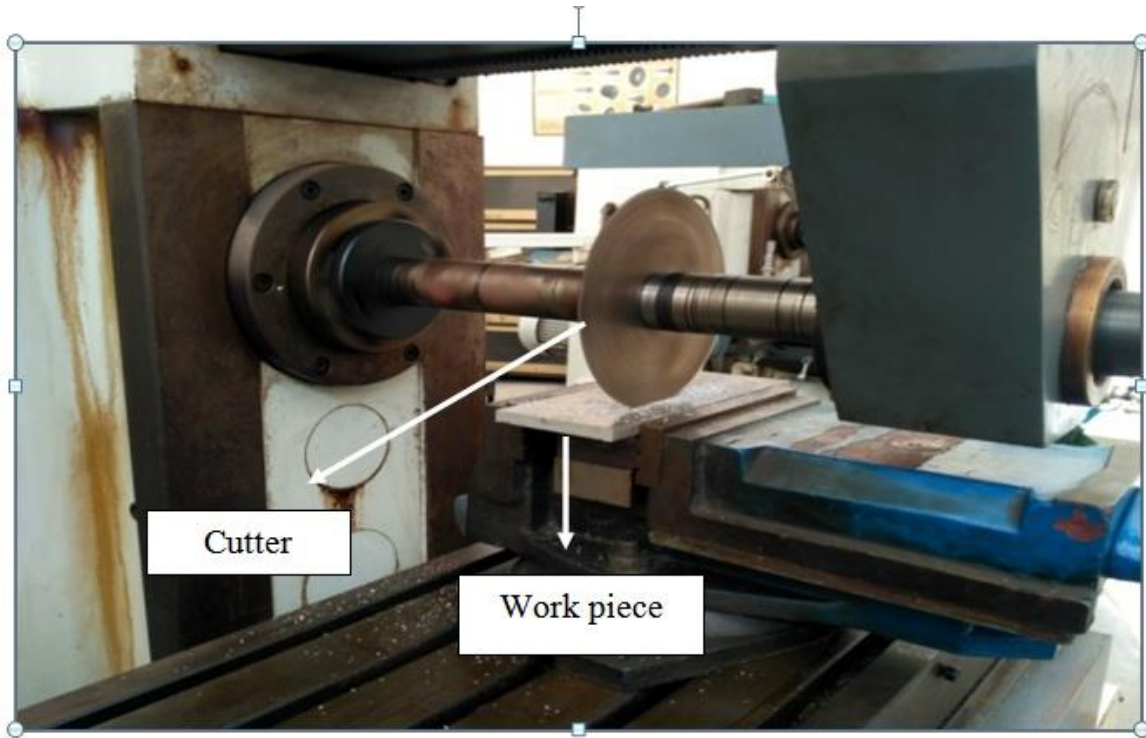
Element	Mg	Si	Mn	Cr	Fe	Cu	Zn	Ti	Al
Comp. (%)	4.5	0.2	0.7	0.09	0.7	0.26	0.04	0.05	Balance



**Figure 3.1: AA 5083 plate used for the experiment**

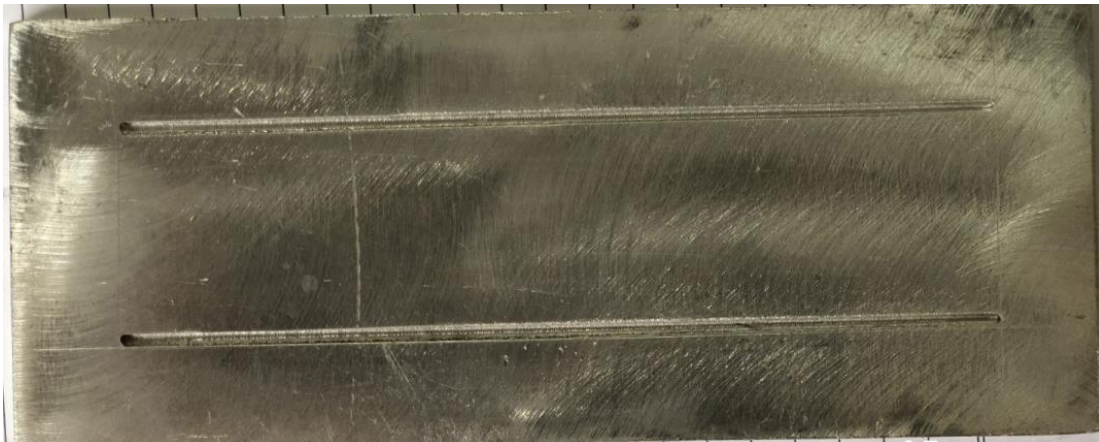
### 3.3 Processing of Workpiece

Grooves were made in the work piece shown in above Figure 3.1 i.e. lengthwise with the help of a milling cutter bought from Sanjay Gandhi Transport Nagar, Delhi. Milling cutter had a bore (inner diameter) of 1.25 inch and outer diameter of 4inch. The Grooves made, were of 2 mm depth and 2mm width, and were spaced at a distance of 30mm from each other to facilitate the specimen testing. The Milling cutter was operated on milling machine present in workshop at Delhi Technological University. The milling machine is shown in following below Figure 3.2.



**Figure 3.2: Grooves were made with the help of milling cutter**

The two grooves produced in a plate with the help of milling cutter. The grooves are shown in following below Figure 3.3.



**Figure 3.3: Grooves without reinforcement on Aluminium 5083 Plate**

### **3.4 Boron Carbide (B<sub>4</sub>C)**

Boron carbide is known to be the third hardest material and is a boron carbon ceramic. It is used in bullet-proof vests and engine sabotage powders. For our experiment Boron Carbide of average particle size less than 60 nano meter was used.



**Figure 3.4: Boron Carbide powder used as reinforcement for the experiment**

### **3.5 Filling of reinforcements in the grooves**

Before filling the reinforcements, the plates were cleaned by keeping them dipped in 500ml of acetone overnight. The fillings of reinforcements have been done considering volume fraction for B<sub>4</sub>C the same was done considering molar solution.

$$\text{Volume Fraction} = \frac{w*d}{t*d_p} \quad (3.5.1)$$

where,

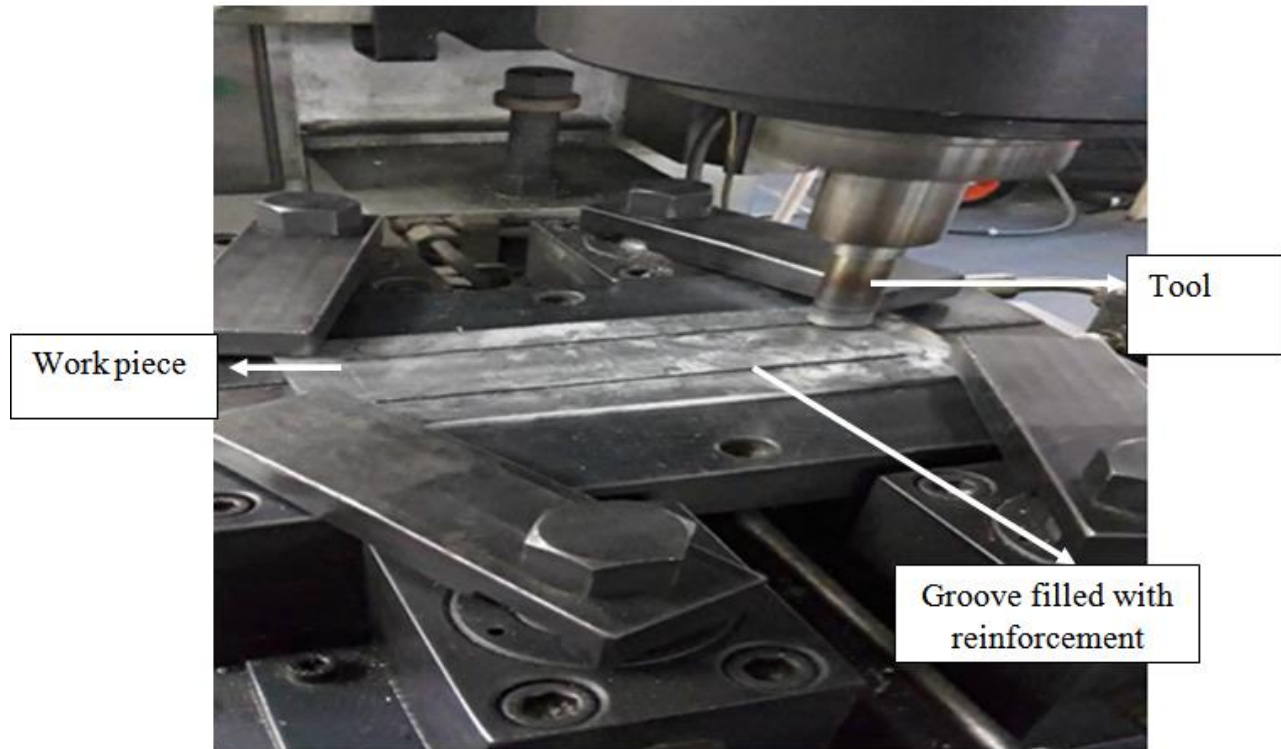
w denotes width of slot cut

d is depth of slot

t is pin length

d<sub>p</sub> is effective diameter of pin

Based on previous research works, volume fraction of 20% was chosen for filling in the slots B<sub>4</sub>C nano particle size, 1 molar solution with diethyl ether was prepared and 5ml solution was poured in each of the slots. Grooves Filled with reinforcement has shown in the Following Figure 3.5.

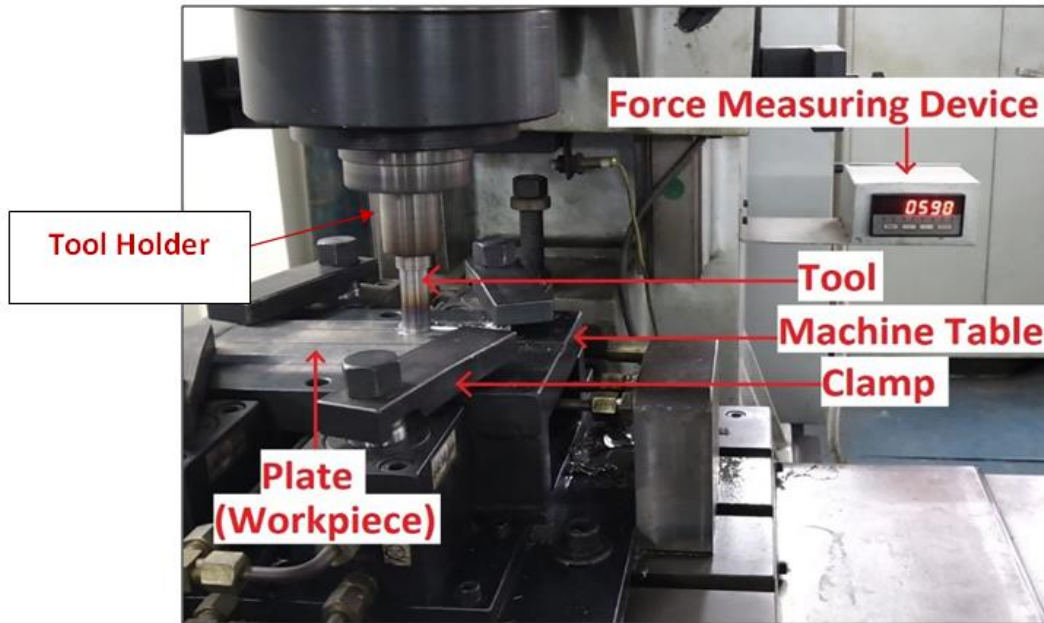


**Figure 3.5: Grooves filled with reinforcement of boron carbide nanoparticle**

### **3.6 FSP Machine Setup**

FSP machine was used for processing of Aluminium alloy 5083. Figure 3.6 shows the FSP machine which was used for fabrication. Table 3.4 shows the full specifications of the FSP machine which was used for fabrication of composite. This machine consists of a 3 phase powerful motor which drives the FSP tool and provides the efficient torque to it. The machine has the system with semi-automatic. It has a hydraulic system which makes it efficient to use and work with accuracy. The hydraulic system was used to clamp the w/p, up and down motion of the tool and the transverse motion of the base. The discharge of the hydraulic was controlled by the actuators using a nob. This affects the motion of the tool and the base plate. In this experiment FSP occurred with the different tool rotational speeds, different tool traverse speed and different number of passes.



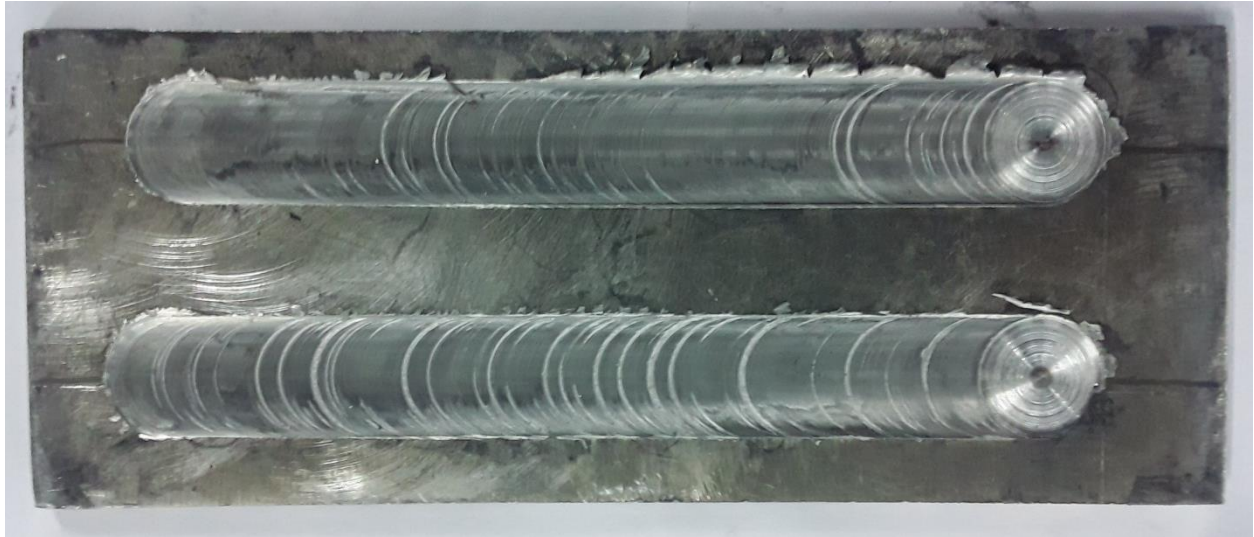


**Figure 3.6: FSP performed in Advanced Metal Joining Lab**

**Table 3.4: FSP Machine full specifications adopted from Advance metal joining lab manual**

<b>Machine Specification</b>	
Machine Size(L×B×H)	1300×1650×2000 mm
Table Working Surface	600×400 mm
Machine Total weight	2 Ton
Welding Materials	MS, Al, Cu
Job Size Maximum (Thickness)	5 mm
Welding Geometry	Straight
<b>Machine travel</b>	
x-axis	600 mm
y-axis	200 mm
z-axis	300 mm
<b>Axis thrust force</b>	
x-axis	250-2500 <u>Kgf</u>
y-axis	400-4000 <u>Kgf</u>
<b>Motion</b>	
x-axis travel speed	0-5000 mm/min
y-axis travel speed	0-2000 mm/min
<b>Spindle Housing</b>	
Spindle	<u>Iso 40 taper</u>
Spindle speed	1440 rpm(max)

Friction stir processing machine in the Advanced Metal Joining Lab, DTU was used to perform the experiment. The experiment was conducted in two phases. In the first phase, capping pass was performed with pin-less tool on each slot to seal the reinforcement. The capping pass plates of AA5083 are shown in the following below Figure3.7.



**Figure 3.7: Capping passes of grooves with probe less tool**

In the second phase, the experiment was conducted in accordance with the design of experiment prepared earlier. The tilt angle for capping pass was kept at  $0^\circ$  while for second phase it was set at  $2^\circ$  based on the previous works. The 20 experiments are performed on the grooves of the AA 5083 plates. The 20 experiments performed on the basis of design matrix in which different TRS, different TTS and different number of passes. When experimentation performed in FSP machine, First of all touches the probe to workpiece and then touches the shoulder to workpiece. For some time tool rubbed the workpiece and produces the heat and plastic deformation occurs due to friction and flow ability starts of the metal. Figure 3.8 shows the all the plastic deformations in the grooves with the help of FSP.



**Figure 3.8: Grooves after the friction stir processing in advance metal joining lab**

### 3.7 Preparation of samples for Tensile Testing

Tensile specimens were prepared from the processed region through CNC wire EDM cutting from Samrat Engineering Works, Samaypur, Delhi. The tensile specimen has prepared as per ASTM E8 subgroup size standard and the samples were taken along the processed surface in the FSP direction with the help of wire EDM machine.



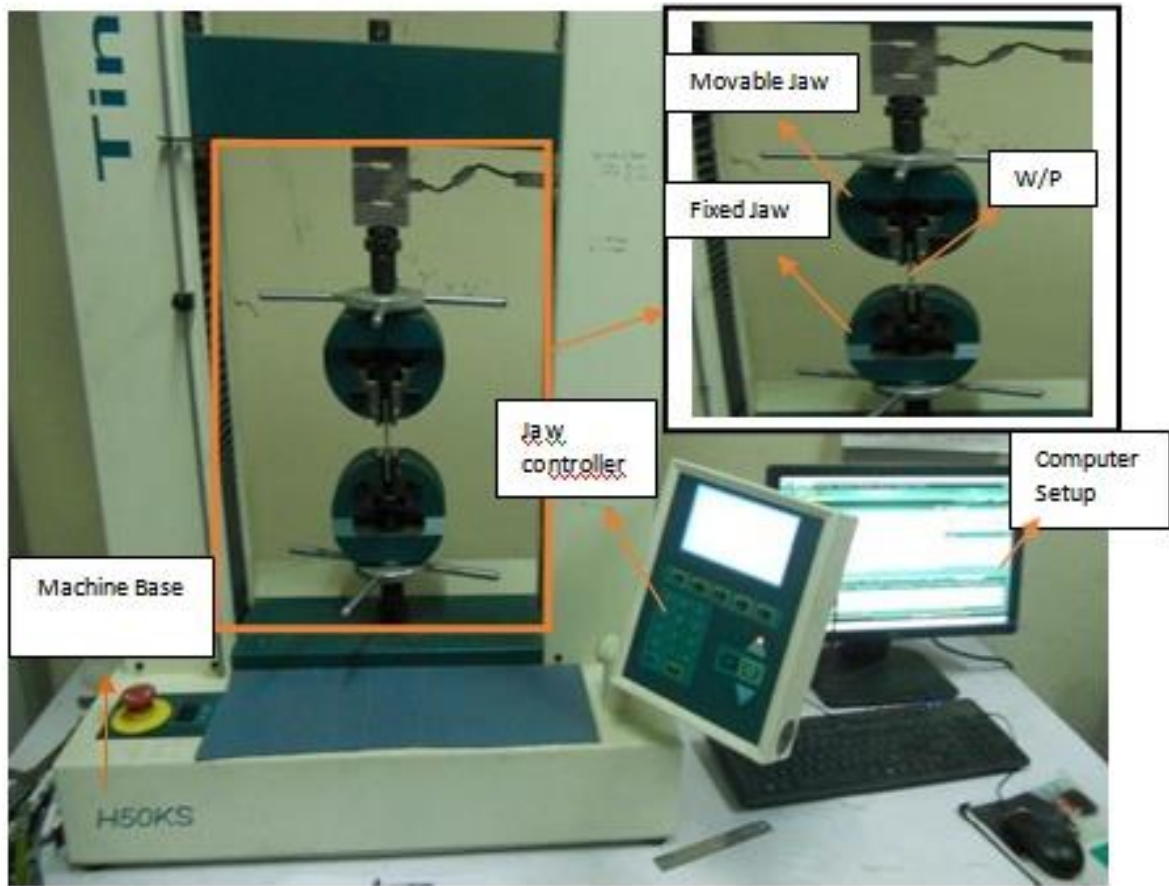


Figure 3.9: Tensile Specimens before testing in UTM machine.



Figure 3.10: Tensile Specimens after Testing in UTM machine.

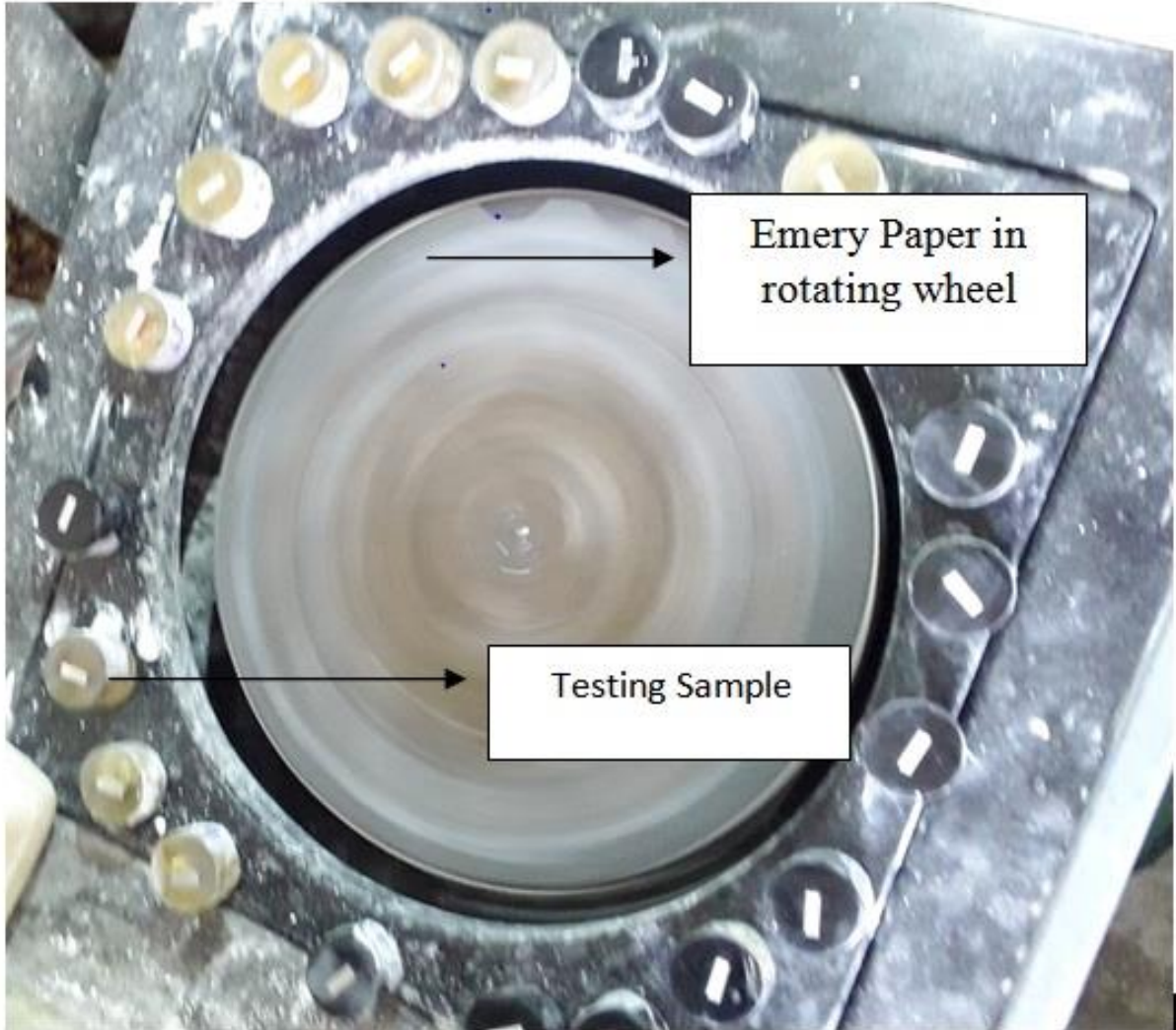
The tensile test has carried out at 1mm/min strain rate at room temperature on computer controlled UTM (Tinius Olsen) H50KS as shown following below in Figure 3.11. UTS, YS and % elongation were recorded.



**Figure 3.11: UTM Machine, DTU**

### **3.8 Preparation of samples for Microstructure and Micro hardness**

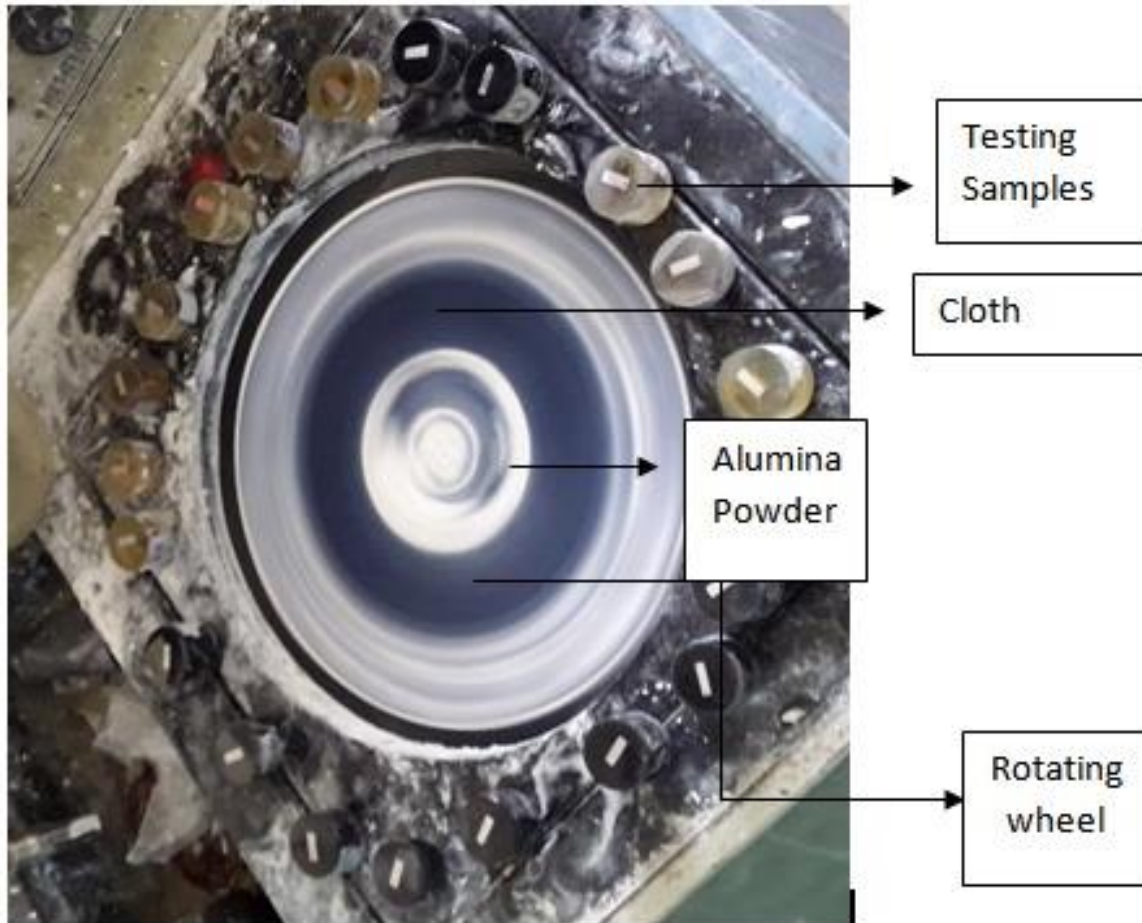
Specimens of dimensions 10mm x 10mm x 4mm were prepared from the processed region through CNC wire EDM cutting from Samrat Engineering Works, Samaypur, Delhi. Cold mounting of the specimens was necessary step to handle of specimens during testing procedures properly. Dry polishing of the specimens was done using different types of emery paper of grit sizes 220,320,400,600,800. Wet polishing was carried out on the emery paper of grit sizes 1000, 1200, 1500 and 2000 with help lubrication of water. The processes are showing following below in the figure 3.12.



**Figure 3.12: Wet polishing on emery paper**

Wet polishing was done on a water lubricated abrasive wheel and used some Alumina powder to obtain smooth surface of specimens. The processes are showing following below in the figure 3.13.





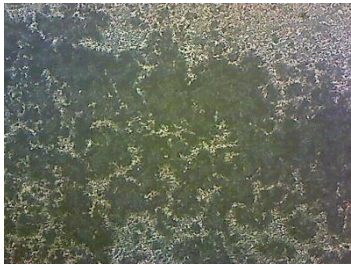
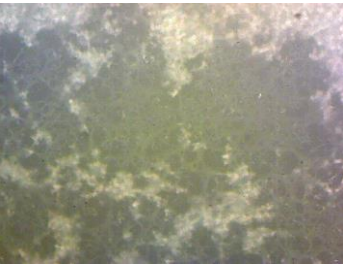


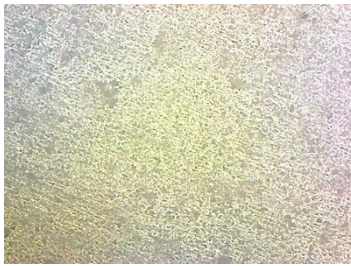
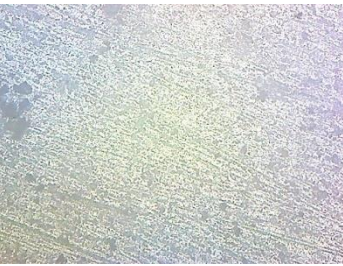
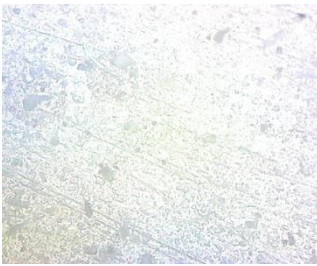
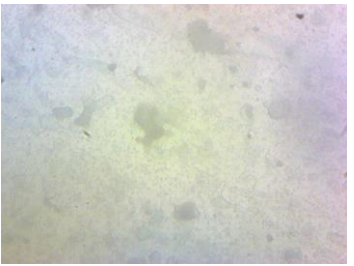

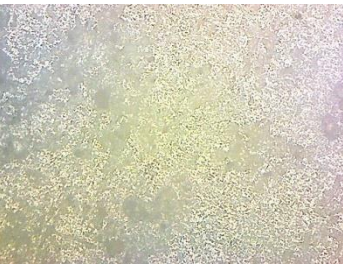
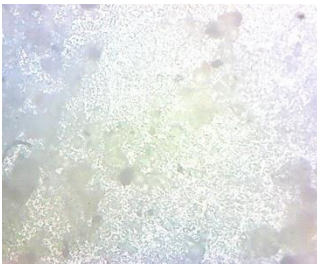
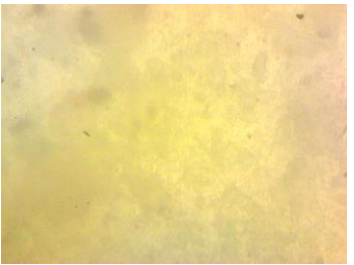



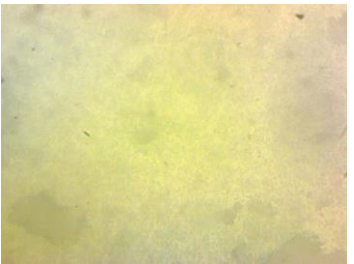
**Figure 3.13: Wet polishing on alumina powder upon the Cloth**

The wet polished specimens were then etched in an acidic medium comprised of Hydrochloric acid and Nitric acid mixed in an optimal molar ratio.




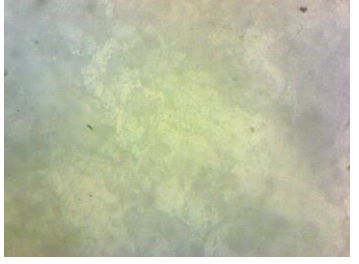
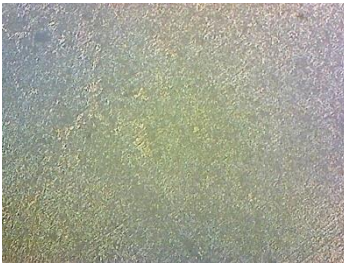
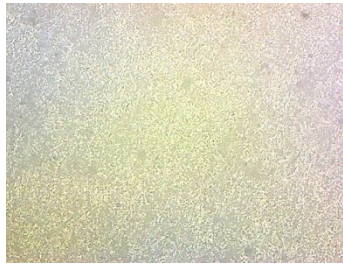
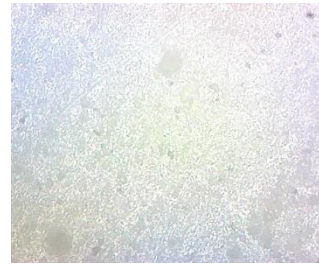
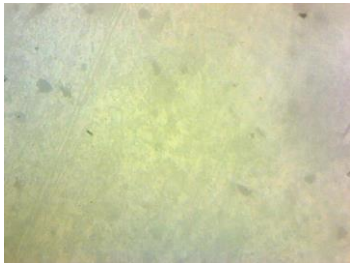
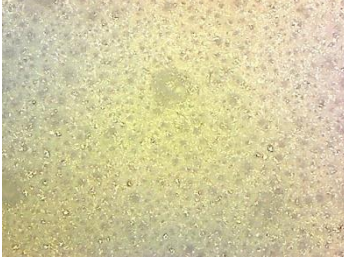


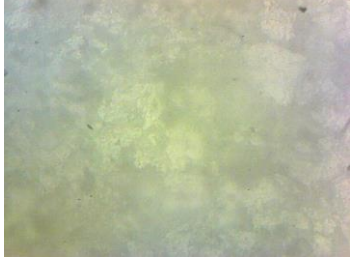
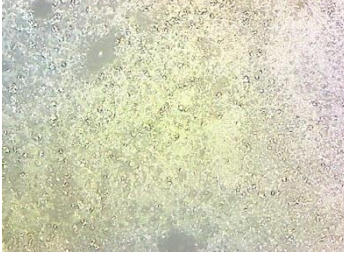



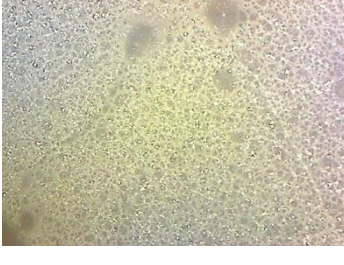


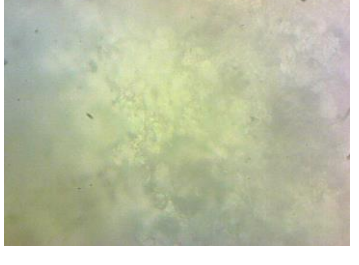
### **3.8.1 Microstructure Testing**

The process of etching helps to identify the presence of grain boundaries when studied under the optical microscope. Grain boundaries are clearly visible with the help of optical microscope. Different magnifications (100x, 200x, 500x and 1000x) are showing different magnified images in the following below Table 3.5.

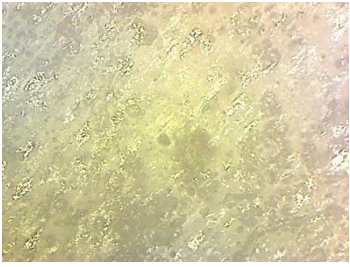
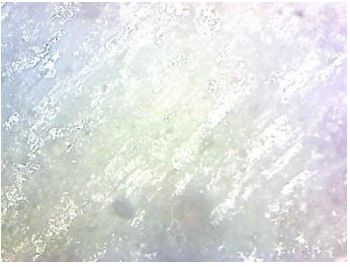

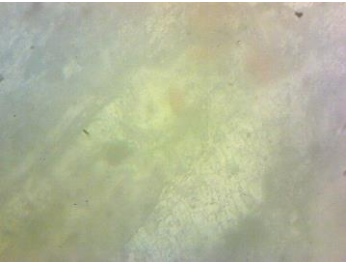



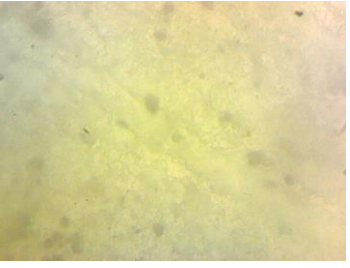



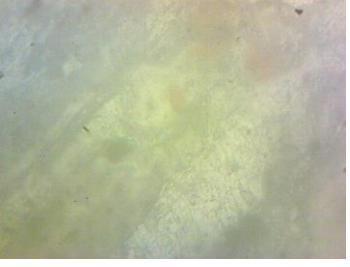
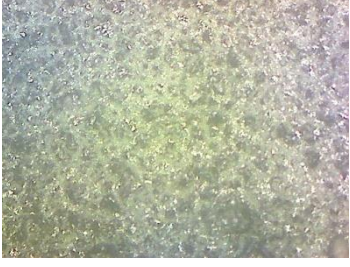

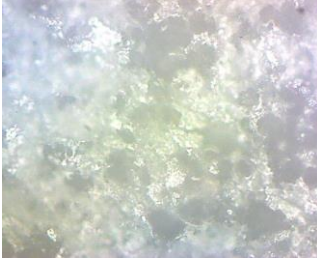
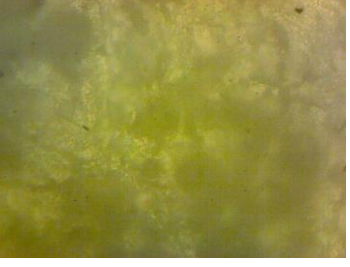



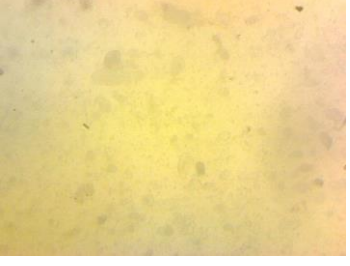
**Table 3.5: Optical microscope images at 100x, 200x, 500x and 1000x of the 20 specimens.**

S.N.	100X	200X	500X	1000X
1				
2				
3				
4				

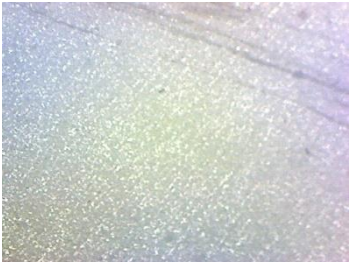


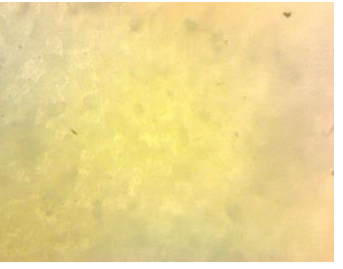




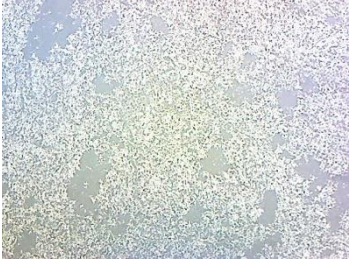

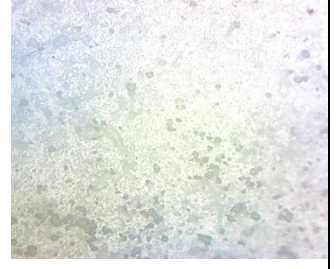
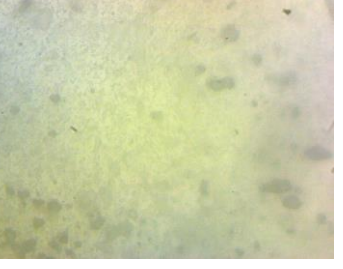






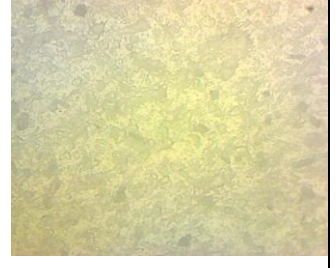
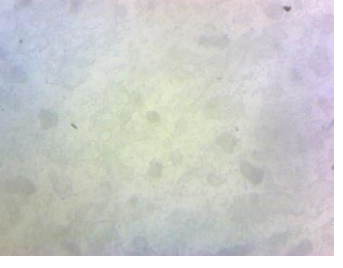


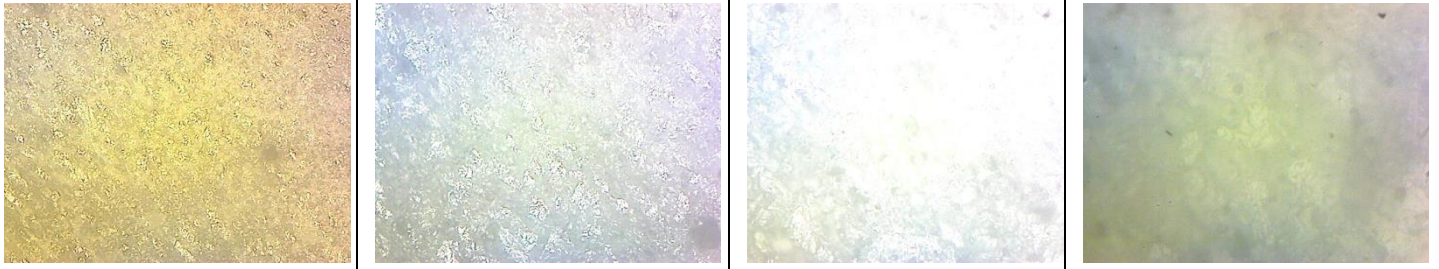
5				
6				
7				
8				
9				



10				
11				
12				
13				
14				

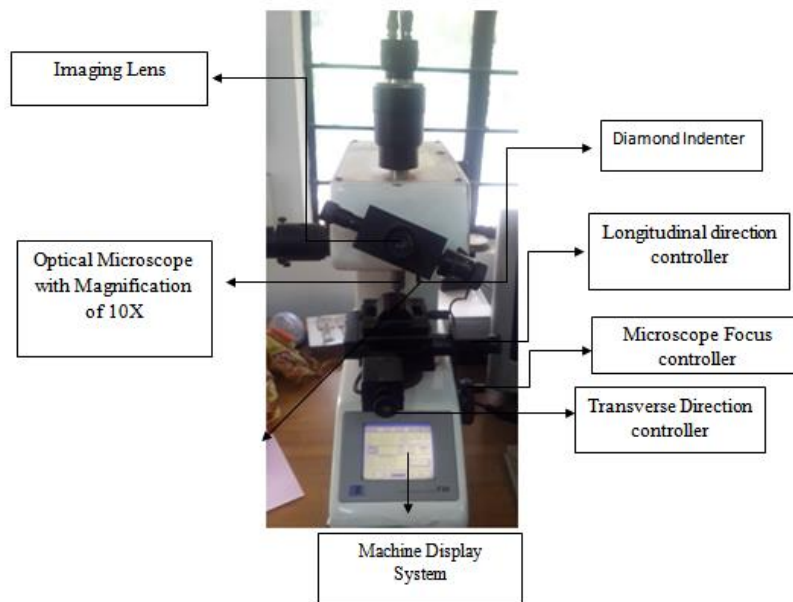


15				
16				
17				
18				
19				



### 3.8.2 Micro Hardness Testing

The Micro hardness test was carried on MICROHARDNESS TESTER FM. Figure 3.14 shows the machine setup. The Vickers micro hardness values were taken using the load of 500gf with a dwell time of the 20s on the processed regions. In this machine first of all alignment of parallel lines are necessary. In this machine have an optical microscope with the magnification of 10 resolutions. In this machine have a diamond indenter i.e. indent the work piece. Then with the help of optical microscope Indentation was clearly visible. Indentation was made in the shape of pyramid. Then measurement of the  $d_1$  i.e. the horizontal distance of pyramid and measurement of the  $d_2$  i.e. the vertical distance of pyramid. Then Machine had displayed the HV value of Vickers Hardness.



**Figure 3.14: Vickers Micro hardness Machine Setup.**

### 3.9 Recording of responses

Recording of responses occurred after the experiments of tensile testing and microhardness. Responses are in this experiment i.e. UTS , YS , % Elongation, Vickers Hardness. All these responses are very important on the basis of mechanical properties. Responses were recorded in Design Expert Software and shown following below in the Table 3.6.

**Table 3.6: Recording of responses**

Std	Run	Coded value of TRS	Coded value of TTS	Coded value of Number of Passes	Actual value of TRS (RPM)	Actual value of TTS (mm/min)	Actual value of Number of Passes (unit)	Response 1 UTS (MPa)	Response 2 YS (MPa)	Response 3 %Elongation (%)	Response 4 Vickers Hardness (HV)
1	9	-1	-1	-1	700	30	1	251	147	17.35	86
2	20	1	-1	-1	1300	30	1	259	158	18.5	89
3	17	-1	1	-1	700	60	1	250	132	17.3	90.1
4	12	1	1	-1	1300	60	1	257	153	17.7	90.7
5	8	-1	-1	1	700	30	3	310	178	24	91.9
6	7	1	-1	1	1300	30	3	328	182	31.5	99.825
7	15	-1	1	1	700	60	3	296	176	27	92
8	1	1	1	1	1300	60	3	313	184	29.1	94.6
9	11	-1	0	0	700	45	2	260	158	18.5	86
10	19	1	0	0	1300	45	2	266	173	21	90

11	5	0	-1	0	1000	30	2	292	171	19.7	91.85
12	2	0	1	0	1000	60	2	282	168	19	93
13	3	0	0	-1	1000	45	1	252	143	17.5	85.8
14	18	0	0	1	1000	45	3	308	179	28	92
15	14	0	0	0	1000	45	2	272	164	18.2	87
16	16	0	0	0	1000	45	2	268	163	18.4	90.85
17	6	0	0	0	1000	45	2	270	162	19	89.6
18	10	0	0	0	1000	45	2	272	161	18.8	88.5
19	4	0	0	0	1000	45	2	271	160	18.9	88.4
20	13	0	0	0	1000	45	2	264	159	20.9	88.15



## CHAPTER 4

### STATISTICAL ANALYSIS

#### 4.1 Introduction

Models are developed on behalf of control system for FSP process to judge surface properties and to construct correlate input parameters like TTS, TRS and Number of passes to UTS, YS and % Elongation. These models are inserted to the computer in order to judge the surface quality for a particular combination of process parameter. The final data was gathered to analyse the non-linearity of models and then the feasibility of the model is judged using ANOVA and plots. Design expert 11.0.6 (Trial version) was used for this purpose.

##### 4.1.1 Developments of statistical models

The output response in relation with input process parameter can be expressed as:-

$$Y = f(\text{TRS, TTS, Number of Passes})$$

Y = Friction Stir Process response;

TRS = Tool Rotational Speed;

TTS = Tool Traverse Speed;

##### 4.1.2 DESIGN EXPERT Trial Version 11.0.6 software

Design expert software is very useful in making leap forward changes to an item or a procedure. We can screen for essential elements, as well as find perfect process settings for top execution and find ideal item details. We can effortlessly see response surfaces from all points with rotatable 3D plots. We can Set flags and investigate forms on intuitive 2D diagrams; and can utilize the numerical enhancement capacity to discover most extreme functions for many reactions simultaneously.

#### 4.2 Investigating the feasibility of the model

ANOVA technique is useful for investigation of the feasibility of the proposed model. According to this method:

1. F ratio marks the platform for evaluating the confidence test, wherein the similarity is tested between the calculated and the reference tabulation.
2. Important condition that relies for feasibility is that Calculated F ratio should always fall short of the reference value, which indicates that model is suitable enough for feasibility. For our analysis, we have assumed the confidence level to be 95%.

##### 4.2.1 Response 1: UTS

**Table 4.1: ANOVA for Reduced Quadratic model of UTS**

Source	Sum of Squares	Df	Mean Square	F-value	p-value	
<b>Model</b>	10011.62	8	1251.45	144.41	< 0.0001	significant
A-TRS	313.60	1	313.60	36.19	< 0.0001	
B-TTS	176.40	1	176.40	20.36	0.0009	
C-Number of Passes	8179.60	1	8179.60	943.86	< 0.0001	
AC	50.00	1	50.00	5.77	0.0351	
BC	84.50	1	84.50	9.75	0.0097	
A <sup>2</sup>	243.46	1	243.46	28.09	0.0003	
B <sup>2</sup>	585.46	1	585.46	67.56	< 0.0001	
C <sup>2</sup>	158.46	1	158.46	18.29	0.0013	
<b>Residual</b>	95.33	11	8.67			
Lack of Fit	47.83	6	7.97	0.8391	0.5881	not significant
Pure Error	47.50	5	9.50			
<b>Cor Total</b>	10106.95	19				

Factor coding is **coded**.

Sum of squares is **Type III – Partial**

The **Model F- value** of 144.41 indicates that the current model under investigation stands significant. Small percentage proportion of occurrence of F value higher could happen on account of noise i.e. 0.01%.

**P value** should not exceed the figure of 0.05 in order to remain significant. It is observed that A, B, C, AC, BC, A<sup>2</sup>, B<sup>2</sup>, C<sup>2</sup> were crucial/significant terms. If the P-values reach above the figure of 0.1; it reflects that model stands insignificant. Thus if the number of insignificant terms are higher in any model, it is recommended to shorten the model by decreasing the parameter in order to enhance the model.

Finally, the Lack of fit F value should remain insignificant for a model in comparison to the pure error. For the current model we achieved 58.81% chance of lack of fit F-value, which could primarily arise due to noise factors.



**Table 4.1.1: Fit Statistics of UTS**

<b>Std. Dev.</b>	2.94	<b>R<sup>2</sup></b>	0.9906
<b>Mean</b>	277.05	<b>Adjusted R<sup>2</sup></b>	0.9837
<b>C.V. %</b>	1.06	<b>Predicted R<sup>2</sup></b>	0.9747
		<b>Adeq Precision</b>	39.4636

The **Predicted R<sup>2</sup>** value is in close approximation with the **Adjusted R<sup>2</sup>** value with a slight variation of 0.2.

**Adeq Precision** enables the user to calculate the S/N ratio. This ratio stands suitable at a desired value of 4 which is 39.464 in our case, thus the signal achieved is quite desirable. Further, this model entitles itself to be satisfiable in the design area.

**Final Equation in Terms of Coded Factors of UTS**

$$UTS = +270.66 + 3.33*A - 2.50*B + 17.01*C + 0.8839*AC - 1.15*BC - 3.33*A^2 + 5.16*B^2 + 2.68*C^2$$

Equations obtained in terms of coded factors are suitable to make assumptions regarding data for given levels of each parameter. Usually, the higher parameters are mark coded as +1 while the lower parameters are referred with -1. Factor coefficient evaluation is beneficial for quantifying the relative effect of the factors in coded equations.

**Final Equation in Terms of Actual Factors of UTS**

$$UTS = +261.70000 + 0.211091*TRS - 5.68303*TTS - 0.346970*\text{Number of Passes} + 0.008333*TRS * \text{Number of Passes} - 0.216667*TTS * \text{Number of Passes} - 0.000105*TRS^2 + 0.064848*TTS^2 + 7.59091*\text{Number of Passes}^2$$

The equation developed on account of actual parameters can be utilised for framing assumption about the output data for given level of each parameter. It is required for each level to be quantified in their respective units for each parameter. This equation should be exempted from examining the relative effect of each parameter as the initial coefficient are magnified to settle up with the units of each parameter while the intercept is not adjusted to the centre of the design area.

**4.2.2 Response 2: YS**

**Table 4.2: ANOVA for Reduced Quadratic model of YS**

<b>Source</b>	<b>Sum of Squares</b>	<b>Df</b>	<b>Mean Square</b>	<b>F-value</b>	<b>p-value</b>	
---------------	-----------------------	-----------	--------------------	----------------	----------------	--

<b>Model</b>	3335.10	7	476.44	58.43	< 0.0001	Significant
A-TRS	348.10	1	348.10	42.69	< 0.0001	
B-TTS	52.90	1	52.90	6.49	0.0256	
C-Number of Passes	2755.60	1	2755.60	337.94	< 0.0001	
AC	50.00	1	50.00	6.13	0.0292	
BC	50.00	1	50.00	6.13	0.0292	
B <sup>2</sup>	76.05	1	76.05	9.33	0.0100	
C <sup>2</sup>	42.05	1	42.05	5.16	0.0424	
<b>Residual</b>	97.85	12	8.15			
Lack of Fit	80.35	7	11.48	3.28	0.1048	not significant
Pure Error	17.50	5	3.50			
<b>Cor Total</b>	3432.95	19				

Factor coding is **coded**.

Sum of squares is **Type III – Partial**

The **Model F-value** of 58.43 indicates that the current model under investigation stands significant. Small percentage proportion of occurrence of F value higher could happen on account of noise i.e. 0.01%.

**P-values** should not exceed the figure of 0.0500 in order to remain significant. It is observed that A, B, C, AC, BC, B<sup>2</sup>, C<sup>2</sup> were crucial/significant terms. If the P-values reach above the figure of 0.1; it reflects that model stands insignificant. Thus if the number of insignificant terms are higher in any model, it is recommended to shorten the model by decreasing the parameter in order to enhance the model.

Finally, the **Lack of fit F value** should remain insignificant for a model in comparison to the pure error. For the current model we achieved 10.48% chance of lack of fit F-value, which could primarily arise due to noise factors. Non-significant lack of fit is good -- we want the model to fit.

**Table 4.2.1: Fit Statistics of YS**

<b>Std. Dev.</b>	2.86	<b>R<sup>2</sup></b>	0.9715
------------------	------	----------------------	--------

<b>Mean</b>	163.55	<b>Adjusted R<sup>2</sup></b>	0.9549
<b>C.V. %</b>	1.75	<b>Predicted R<sup>2</sup></b>	0.8824
		<b>Adeq Precision</b>	27.6854

The **Predicted R<sup>2</sup>** value is in close approximation with the **Adjusted R<sup>2</sup>** value with a slight variation of 0.2.

**Adeq Precision** enables the user to calculate the S/N ratio. This ratio stands suitable at a desired value of 4 which is 27.6854 in our case, thus the signal achieved is quite desirable. Further, this model entitles itself to be satisfiable in the design area.

#### **Final Equation in Terms of Coded Factors of YS**

$$YS = +162.92 + 3.51*A - 1.37*B + 9.87*C - 0.8839*AC + 0.8839*BC + 1.72*B^2 - 1.28*C^2$$

Equations obtained in terms of coded factors are suitable to make assumptions regarding data for given levels of each parameter. Usually, the higher parameters are mark coded as +1 while the lower parameters are referred with -1. Factor coefficient evaluation is beneficial for quantifying the relative effect of the factors in coded equations.

#### **Final Equation in Terms of Actual Factors of YS**

$$YS = +144.66667 + 0.036333*TRS - 2.43667*TTS + 31.93333*Number\ of\ Passes - 0.008333*TRS * Number\ of\ Passes + 0.166667*TTS * Number\ of\ Passes + 0.021667*TTS^2 - 3.62500*Number\ of\ Passes^2$$

The equation developed on account of actual parameters can be utilised for framing assumption about the output data for given level of each parameter. It is required for each level to be quantified in their respective units for each parameter. This equation should be exempted from examining the relative effect of each parameter as the initial coefficient are magnified to settle up with the units of each parameter while the intercept is not adjusted to the centre of the design area.

#### **4.2.3 Response 3: % Elongation**

**Table 4.3: ANOVA for Reduced Quadratic model of % Elongation**

<b>Source</b>	<b>Sum of Squares</b>	<b>df</b>	<b>Mean Square</b>	<b>F-value</b>	<b>p-value</b>	
<b>Model</b>	357.40	6	59.57	89.42	< 0.0001	Significant
A-TRS	18.63	1	18.63	27.97	0.0001	
B-TTS	0.0903	1	0.0903	0.1355	0.7187	

C-Number of Passes	262.66	1	262.66	394.32	< 0.0001	
AB	4.73	1	4.73	7.10	0.0195	
AC	8.10	1	8.10	12.16	0.0040	
C <sup>2</sup>	63.19	1	63.19	94.87	<0.0001	
<b>Residual</b>	8.66	13	0.6661			
Lack of Fit	4.01	8	0.5008	0.5381	0.7923	not significant
Pure Error	4.65	5	0.9307			
<b>Cor Total</b>	366.06	19				

Factor is **Coded**.

Sum of squares is **Type III – Partial**

The **Model F-value** of 89.42 indicates that the current model under investigation stands significant. Small percentage proportion of occurrence of F value higher could happen on account of noise i.e. 0.01%.

**P value** should not exceed the figure of 0.05 in order to remain significant. It is observed that A, B, C, AB, AC, C<sup>2</sup> were crucial/significant terms. If the P-values reach above the figure of 0.1; it reflects that model stands insignificant. Thus if the number of insignificant terms are higher in any model, it is recommended to shorten the model by decreasing the parameter in order to enhance the model.

Finally, the **Lack of fit F value** should remain insignificant for a model in comparison to the pure error. For the current model we achieved 79.23% chance of lack of fit F-value, which could primarily arise due to noise factors. Non-significant lack of fit is good -- we want the model to fit.

**Table 4.3.1: Fit Statistics of % Elongation**

<b>Std. Dev.</b>	0.8162	<b>R<sup>2</sup></b>	0.9763
<b>Mean</b>	21.02	<b>Adjusted R<sup>2</sup></b>	0.9654
<b>C.V. %</b>	3.88	<b>Predicted R<sup>2</sup></b>	0.9131
		<b>Adeq Precision</b>	30.0667

The **Predicted R<sup>2</sup>** value is in close approximation with the **Adjusted R<sup>2</sup>** value with a slight variation of 0.2.

**Adeq Precision** enables the user to calculate the S/N ratio. This ratio stands suitable at a desired value of 4 which is 30.0667 in our case, thus the signal achieved is quite desirable. Further, this model entitles itself to be satisfiable in the design area.

**Final Equation in Terms of Coded Factors of % Elongation**

$$\% \text{ Elongation} = +19.24 + 0.8116 * A - 0.0565 * B + 3.05 * C - 0.2718 * AB + 0.3558 * AC + 1.26 * C^2$$

Equations obtained in terms of coded factors are suitable to make assumptions regarding data for given levels of each parameter. Usually, the higher parameters are mark coded as +1 while the lower parameters are referred with -1. Factor coefficient evaluation is beneficial for quantifying the relative effect of the factors in coded equations.

**Final Equation in Terms of Actual Factors of % Elongation**

$$\% \text{ Elongation} = +17.96583 + 0.005529 * \text{TRS} + 0.164500 * \text{TTS} - 12.44917 * \text{Number of Passes} - 0.000171 * \text{TRS} * \text{TTS} + 0.003354 * \text{TRS} * \text{Number of Passes} + 3.55500 * \text{Number of Passes}^2$$

The equation developed on account of actual parameters can be utilised for framing assumption about the output data for given level of each parameter. It is required for each level to be quantified in their respective units for each parameter. This equation should be exempted from examining the relative effect of each parameter as the initial coefficient are magnified to settle up with the units of each parameter while the intercept is not adjusted to the centre of the design area.

**4.2.4 Response 4: Vickers Hardness**

**Table 4.4: ANOVA for Reduced Quadratic model of Vickers Hardness**

Source	Sum of Squares	df	Mean Square	F-value	p-value	
<b>Model</b>	197.45	7	28.21	27.90	< 0.0001	Significant
A-TRS	32.85	1	32.85	32.49	< 0.0001	
B-TTS	0.3331	1	0.3331	0.3294	0.5766	
C-Number of Passes	82.51	1	82.51	81.60	< 0.0001	
AB	7.46	1	7.46	7.38	0.0187	
AC	5.99	1	5.99	5.93	0.0315	
BC	14.92	1	14.92	14.76	0.0023	
B <sup>2</sup>	53.38	1	53.38	52.80	< 0.0001	

<b>Residual</b>	12.13	12	1.01			
Lack of Fit	3.39	7	0.4848	0.2773	0.9378	not significant
Pure Error	8.74	5	1.75			
<b>Cor Total</b>	209.59	19				

Factor coding is **Coded**.

Sum of squares is **Type III - Partial**

The **Model F-value** of 27.90 indicates that the current model under investigation stands significant. Small percentage proportion of occurrence of F value higher could happen on account of noise i.e. 0.01%.

**P value** should not exceed the figure of 0.05 in order to remain significant. It is observed that A, B, C, AB, AC, BC, B<sup>2</sup> were crucial/significant terms. If the P-values reach above the figure of 0.1; it reflects that model stands insignificant. Thus if the number of insignificant terms are higher in any model, it is recommended to shorten the model by decreasing the parameter in order to enhance the model.

Finally, the **Lack of fit F value** should remain insignificant for a model in comparison to the pure error. For the current model we achieved 93.78% chance of lack of fit F-value, which could primarily arise due to noise factors. Non-significant lack of fit is good -- we want the model to fit.

**Table 4.4.1: Fit Statistics of Vickers Hardness**

<b>Std. Dev.</b>	1.01	<b>R<sup>2</sup></b>	0.9421
<b>Mean</b>	90.26	<b>Adjusted R<sup>2</sup></b>	0.9083
<b>C.V. %</b>	1.11	<b>Predicted R<sup>2</sup></b>	0.8080
		<b>Adeq Precision</b>	22.0649

The **Predicted R<sup>2</sup>** value is in close approximation with the **Adjusted R<sup>2</sup>** value with a slight variation of 0.2.

**Adeq Precision** enables the user to calculate the S/N ratio. This ratio stands suitable at a desired value of 4 which is 22.0649 in our case, thus the signal achieved is quite desirable. Further, this model entitles itself to be satisfiable in the design area.

**Final Equation in Terms of Coded Factors of Vickers Hardness**

$$\text{Vickers Hardness} = +88.63 + 1.08*A + 0.1085*B + 1.71*C - 0.3414*AB + 0.3060*AC - 0.4828*BC + 1.16*B^2$$

Equations obtained in terms of coded factors are suitable to make assumptions regarding data for given levels of each parameter. Usually, the higher parameters are mark coded as +1 while the lower parameters are referred with -1. Factor coefficient evaluation is beneficial for quantifying the relative effect of the factors in coded equations.

#### **Final Equation in Terms of Actual Factors of Vickers Hardness**

$$\text{Vickers Hardness} = +93.62417 + 0.009927*TRS - 0.898167*TTS + 4.08396*\text{Number of Passes} - 0.000215*TRS * TTS + 0.002885*TRS * \text{Number of Passes} - 0.091042*TTS * \text{Number of Passes} + 0.014522*TTS^2$$

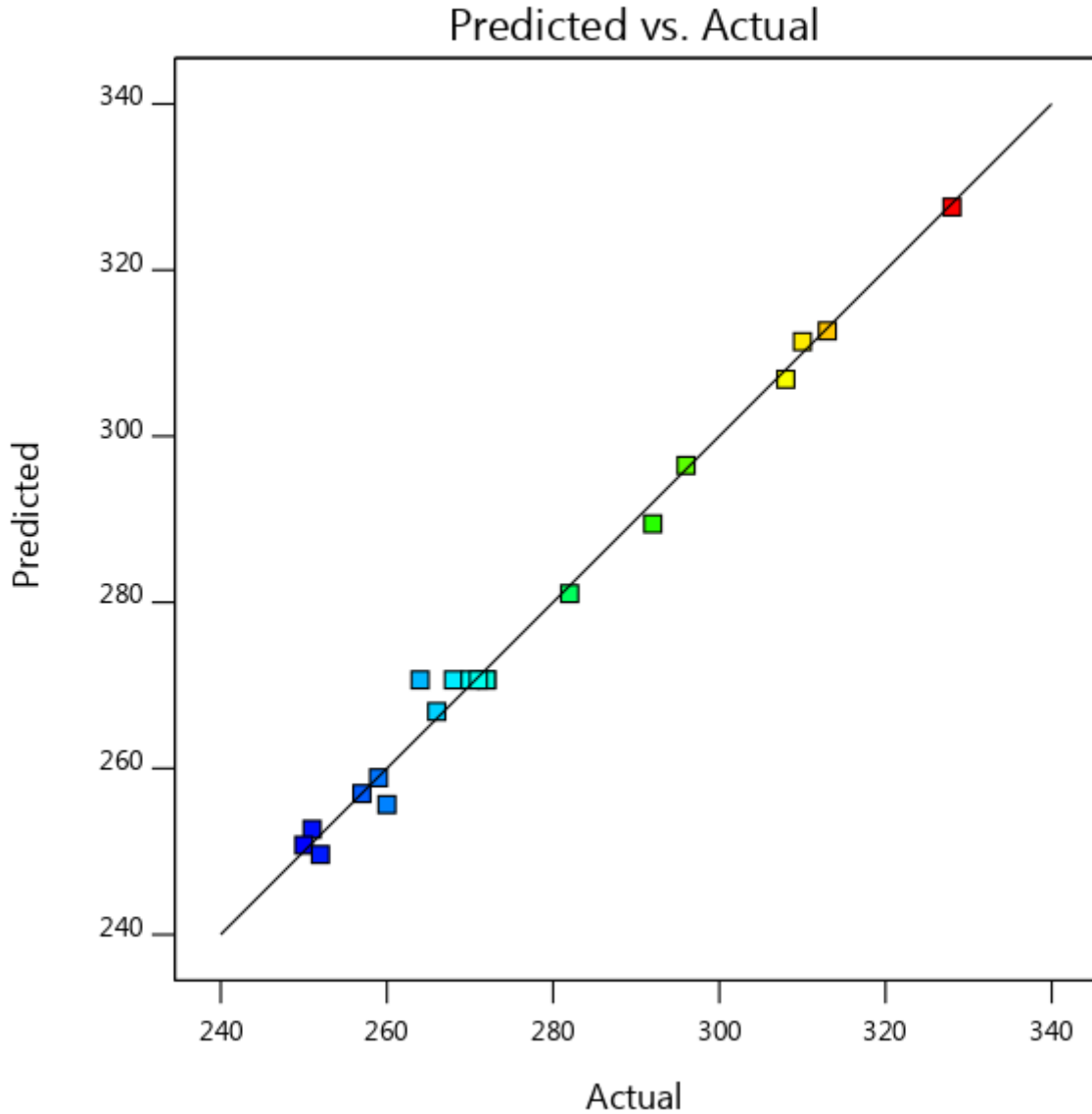
The equation in terms of actual factors can be used to make predictions about the response for given levels of each factor. Here, the levels should be specified in the original units for each factor. This equation should not be used to determine the relative impact of each factor because the coefficients are scaled to accommodate the units of each factor and the intercept is not at the center of the design space.

## CHAPTER 5

### RESULT ANALYSIS AND DISCUSSION

#### 5.1 Analysis of Result

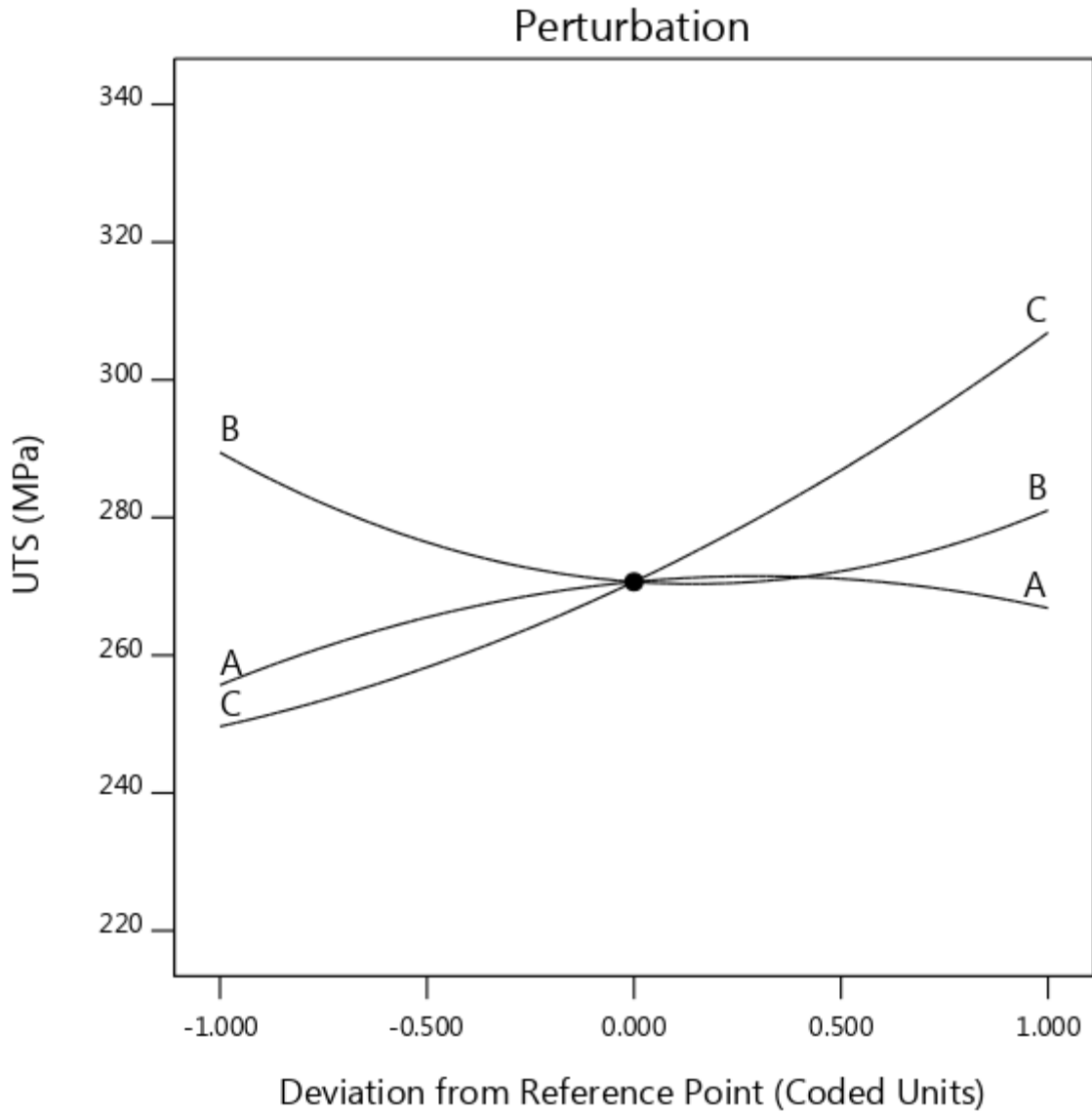
##### 5.1.1 Effect of analysis on UTS



**Figure 5.1: Graph between Predicted vs. Actual points of UTS**

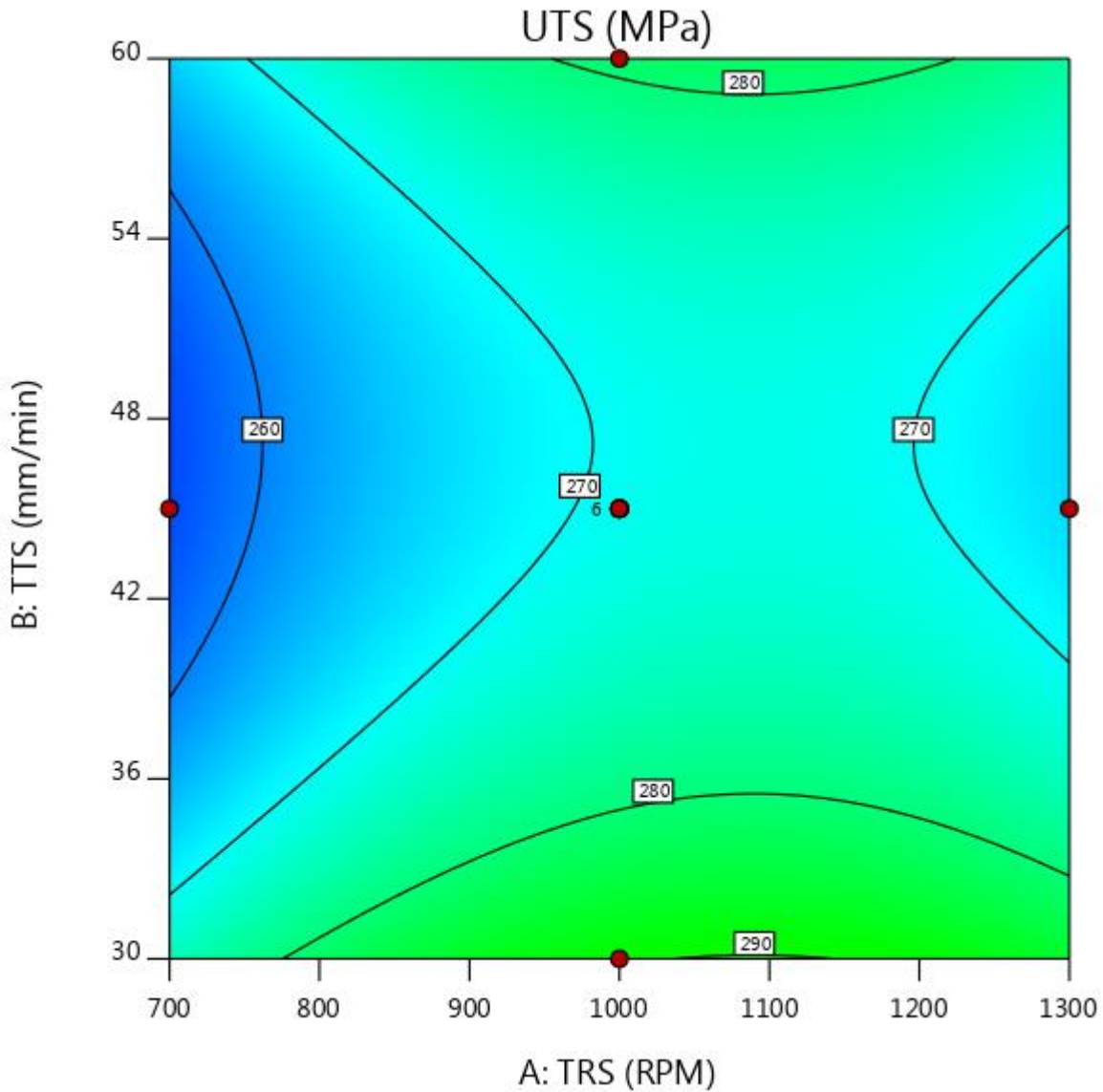
The above graph depicts actual data of UTS on x-axis while predicted data of UTS on the y-axis. Red dots represent highest value of UTS while a blue dot represents the least values of UTS. From the graph, it is evident that actual data approaches similarity to predicted data. The graph shows that correlation between Predicted and Actual data points.





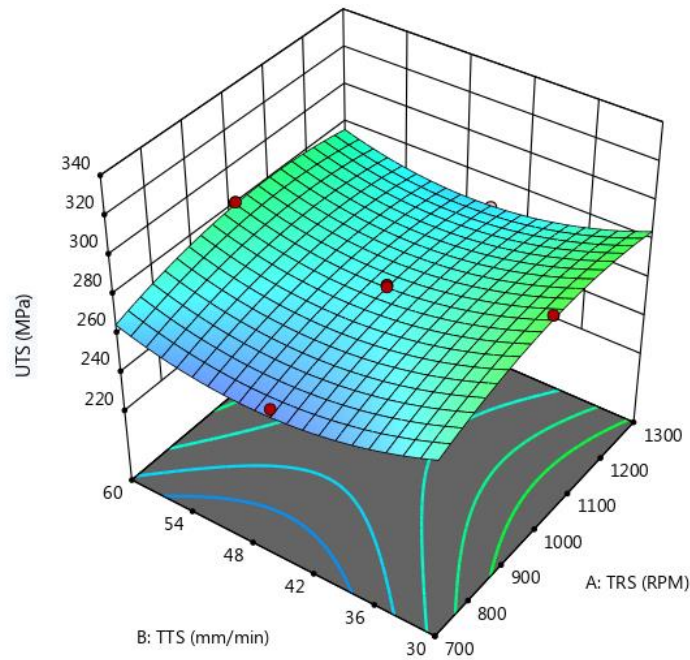
**Figure 5.2 Graph represents the intersection point of UTS**

The above graph depicts deviation from reference point on x-axis while UTS on the y-axis. This graph is called perturbation curve. In this graph, 3 different coding factors named as A, B and C are intersecting at a point.



**Figure 5.3: Contour plot of UTS between TRS and TTS**

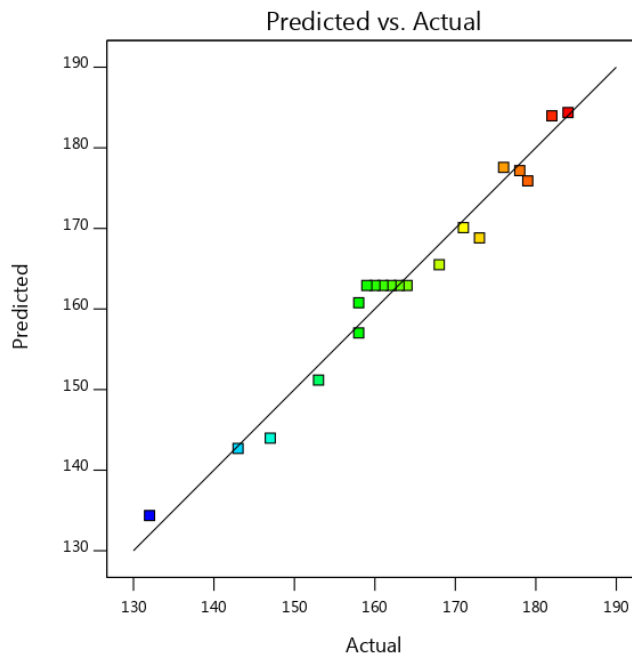
This graph depicts, TRS (RPM) on the x-axis while TTS (mm/min) on the y-axis. On this curve, UTS point is achieved. Red areas represent maximum value (328MPa) of UTS while blue areas represent the minimum values of UTS (250 MPa). Contour plots describe the 2-D response surfaces. Contour plots have a crucial part in investigating of the response surfaces. Once created through Software, the profile of surface can be predicted and optimized values are achieved with precision.



**Figure 5.4: 3 D response surface graph of UTS between TRS and TTS**

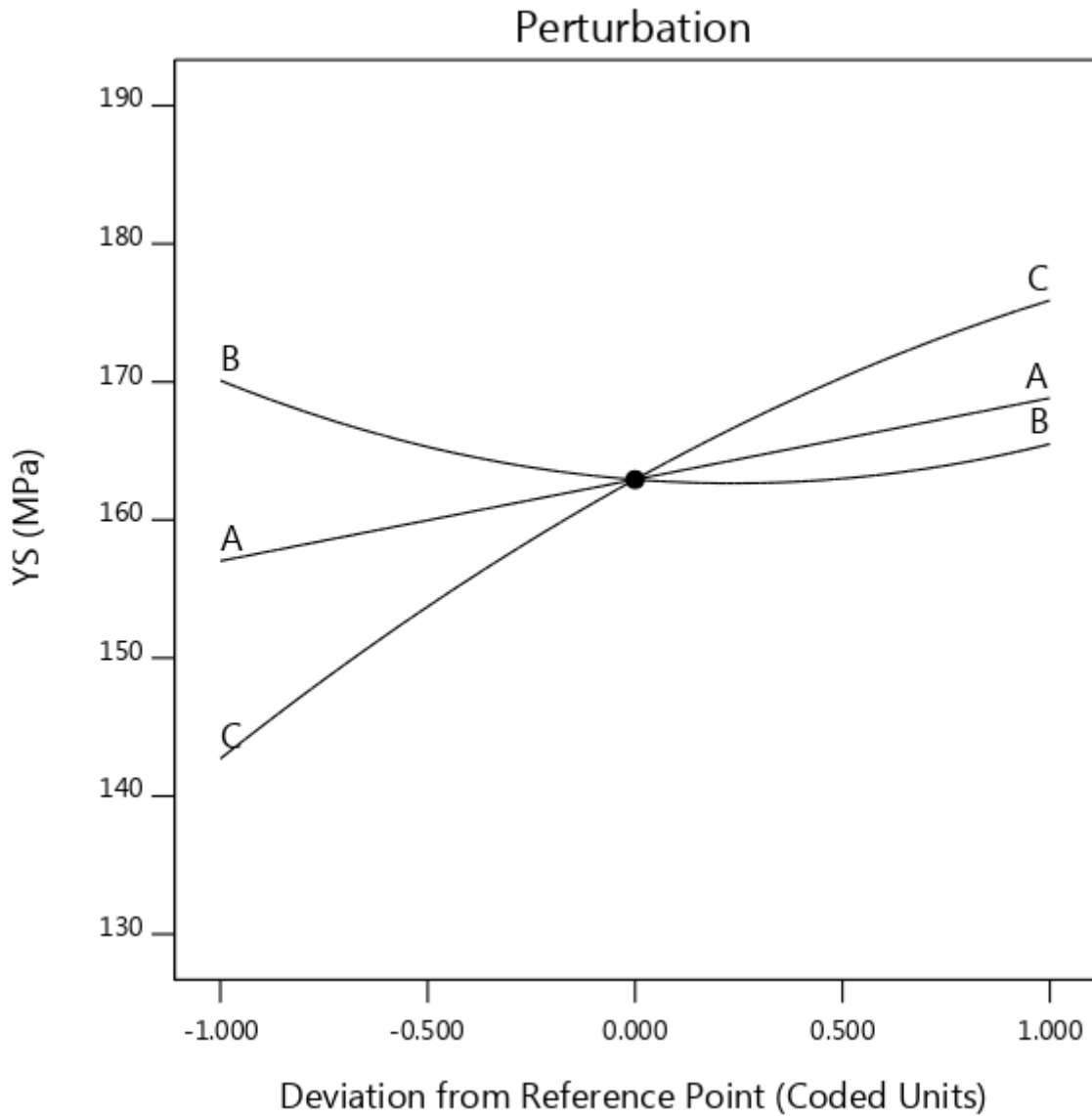
This graph depicts TRS as x1-axis while TTS on the x2-axis, finally UTS on y-axis. Response surface geometry is 3-D in nature.

**5.1.2 Effect of analysis on YS**



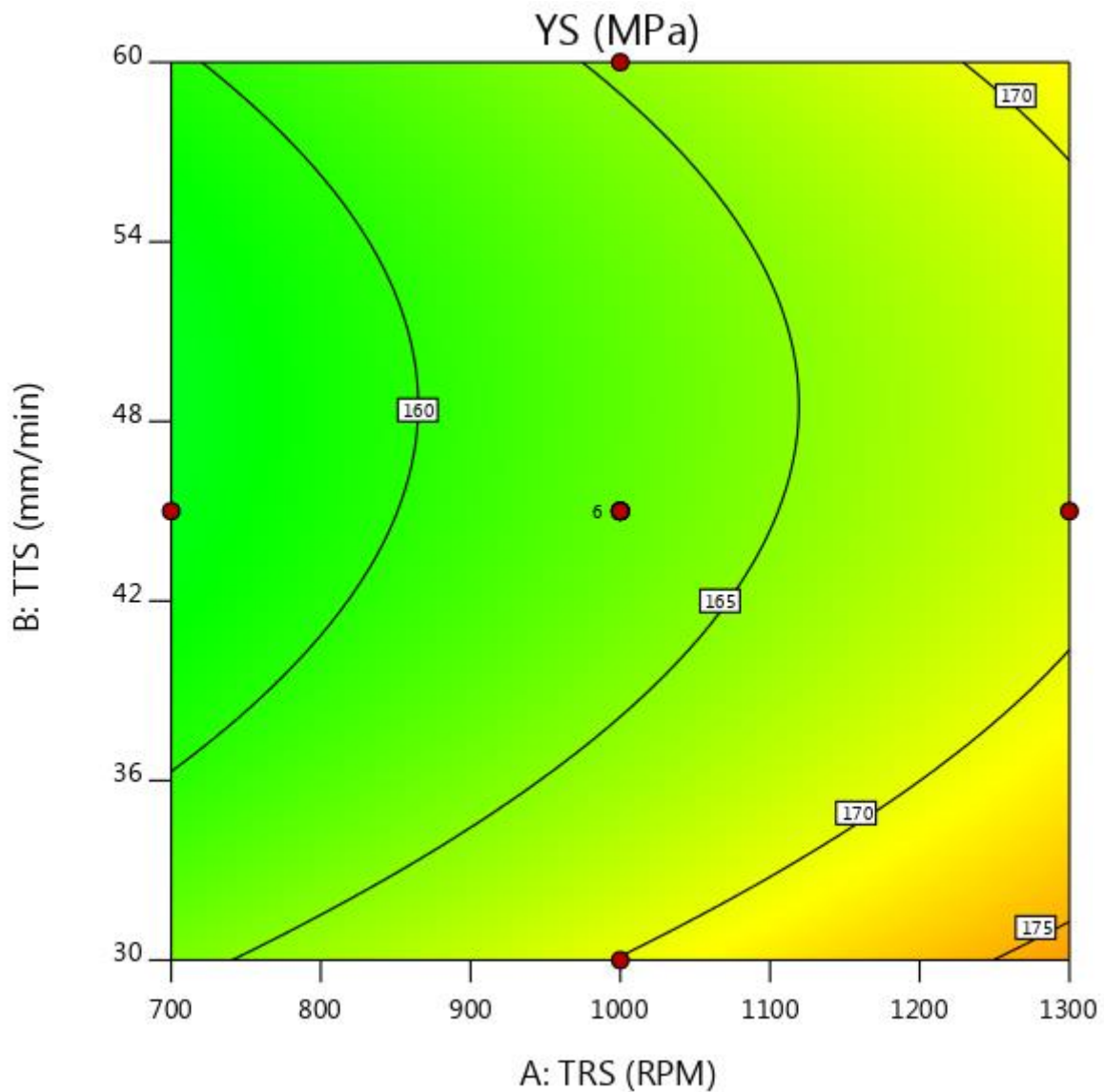
**Figure 5.5: Graph between Predicted vs Actual points of YS**

The above graph depicts actual data of YS on x-axis while predicted data of YS on the y-axis. Red dots represent highest value of YS while a blue dot represents the least values of YS. From the graph, it is evident that actual data approaches similarity to predicted data.



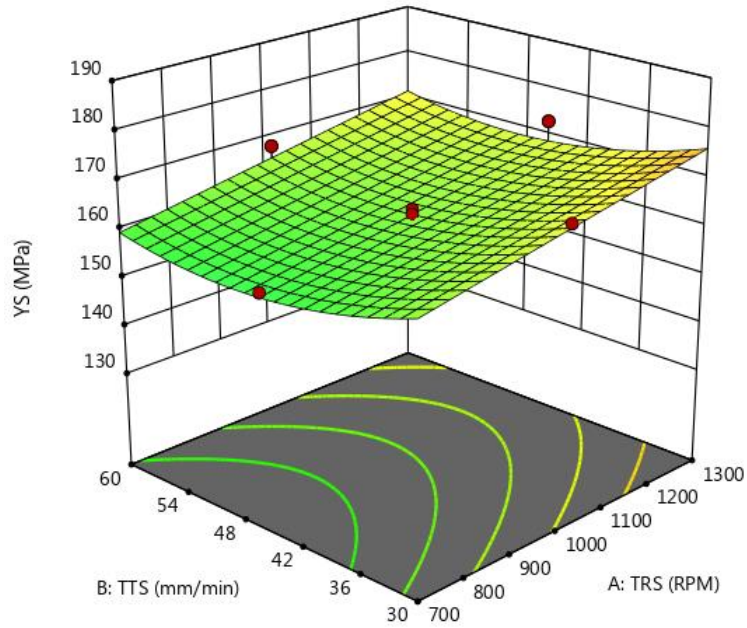
**Figure 5.6: Graph represents the intersection point of YS**

The above graph depicts deviation from reference point on x-axis while YS on the y-axis. This graph is called perturbation curve. In this graph, 3 different coding factors named as A, B and C are intersecting at a point.



**Figure 5.7: Contour Plot of YS between TRS and TTS**

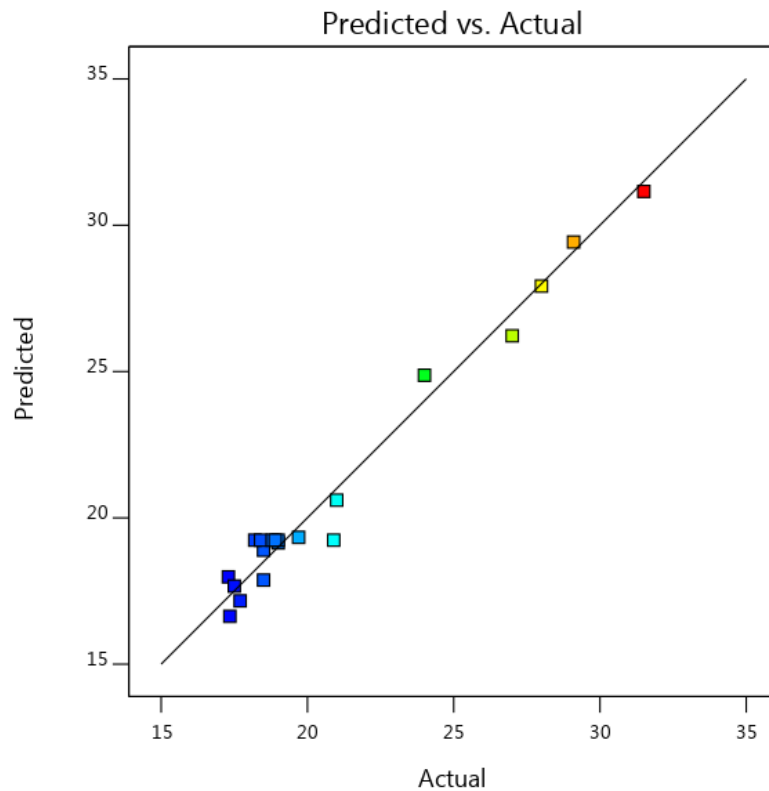
This graph depicts, TRS (RPM) on the x-axis while TTS (mm/min) on the y-axis. On this curve, YS point is achieved. Red areas represent maximum value (184MPa) of YS while blue areas represent the minimum values of YS (132MPa). Contour plots describe the 2-D response surfaces. Contour plots have a crucial part in investigating of the response surfaces. Once created through Software, the profile of surface can be predicted and optimized values are achieved with precision.



**Figure 5.8: 3 D response surface graph of YS between TRS and TTS**

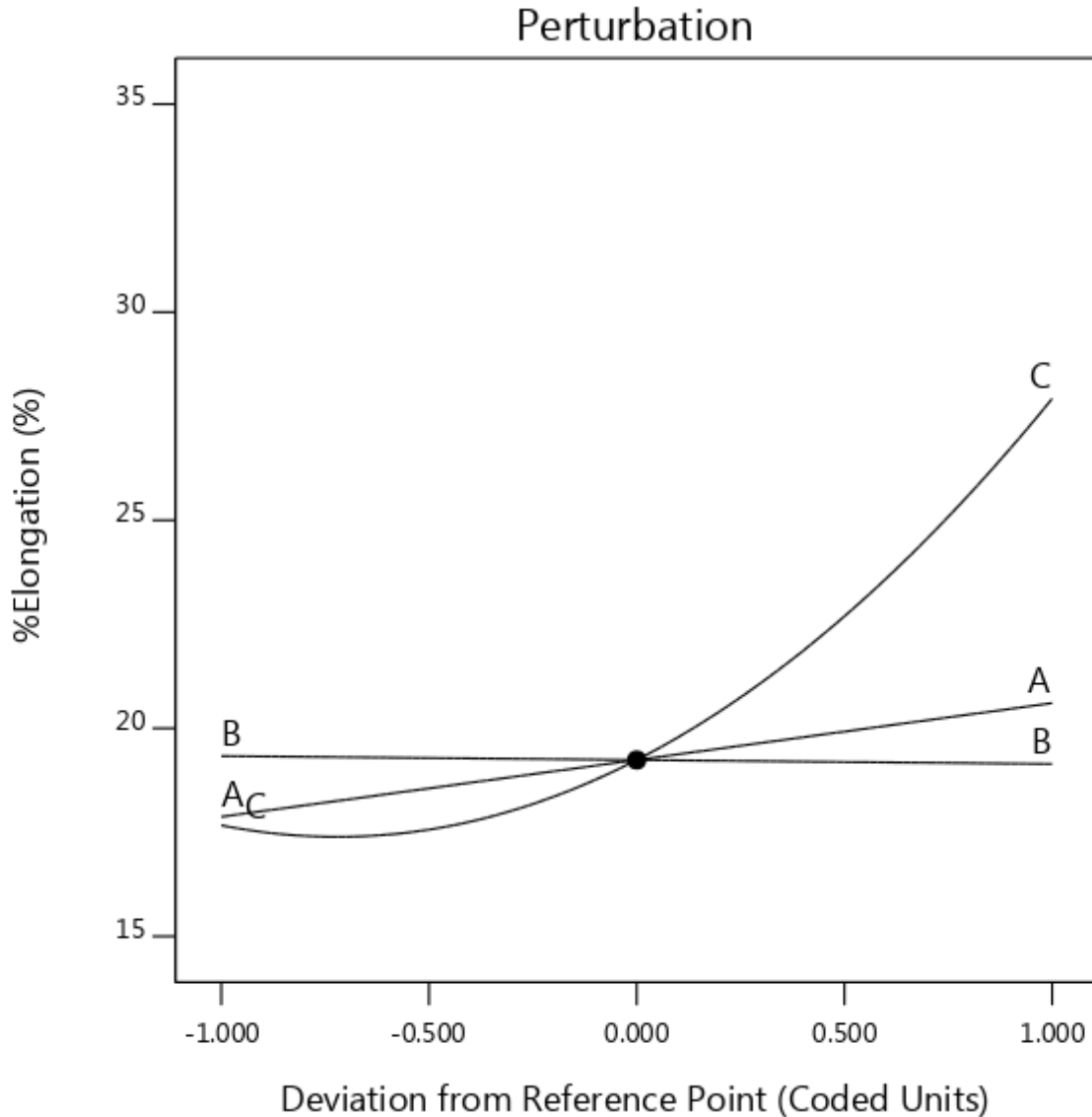
This graph depicts TRS as x1-axis while TTS on the x2-axis, finally YS on y-axis. Response surface geometry is 3-D in nature.

### 5.1.3 Effect of analysis on % Elongation



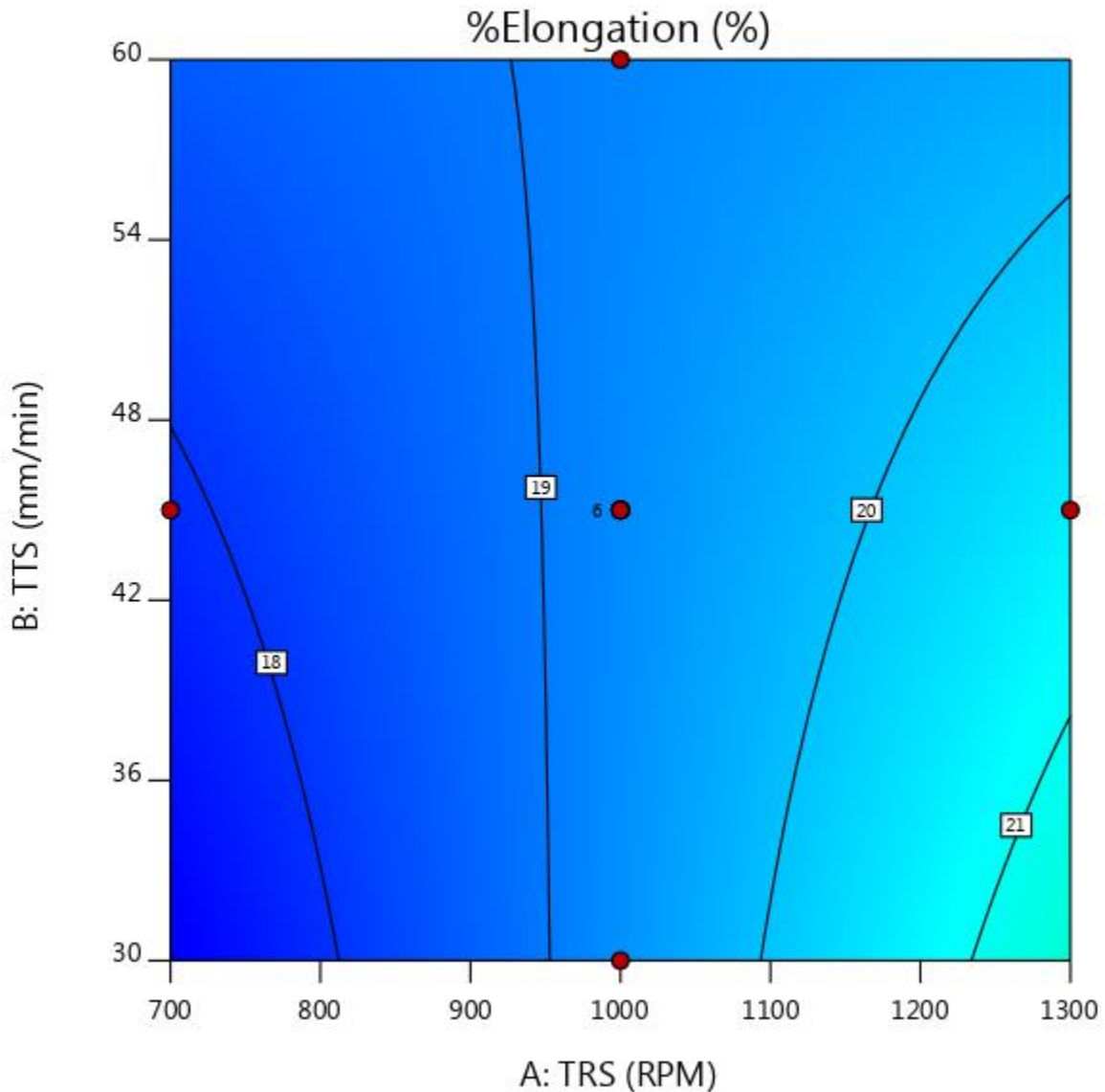
**Figure 5.9: Graph between Predicted vs Actual points of % Elongation.**

The above graph depicts actual data of % Elongation on x-axis while predicted data of % Elongation on the y-axis. Red dots represent highest value of % Elongation while a blue dot represents the least values of % Elongation. From the graph, it is evident that actual data approaches similarity to predicted data.



**Figure 5.10: Graph represents the intersection point of % Elongation**

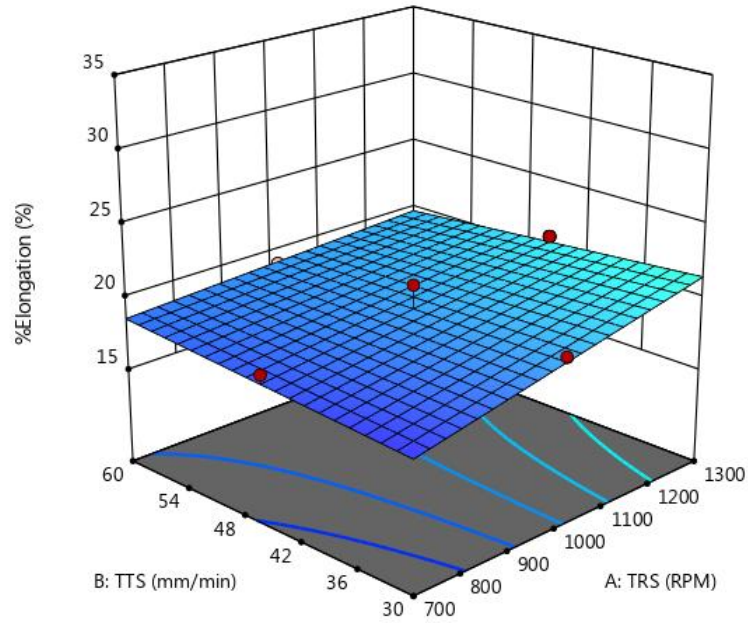
The above graph depicts deviation from reference point on x-axis while % Elongation on the y-axis. This graph is called perturbation curve. In this graph, 3 different coding factors named as A, B and C are intersecting at a point.



**Figure 5.11: Contour Plot of % Elongation between TRS and TTS**

This graph depicts, TRS (RPM) on the x-axis while TTS (mm/min) on the y-axis. On this curve, % Elongation point is achieved. Red areas represent maximum value (17.3%) of % Elongation while blue areas represent the minimum values of % Elongation (31.5%). Contour plots describe the 2-D response surfaces. Contour plots have a crucial part in investigating of the response surfaces. Once created through Software, the profile of surface can be predicted and optimized values are achieved with precision.

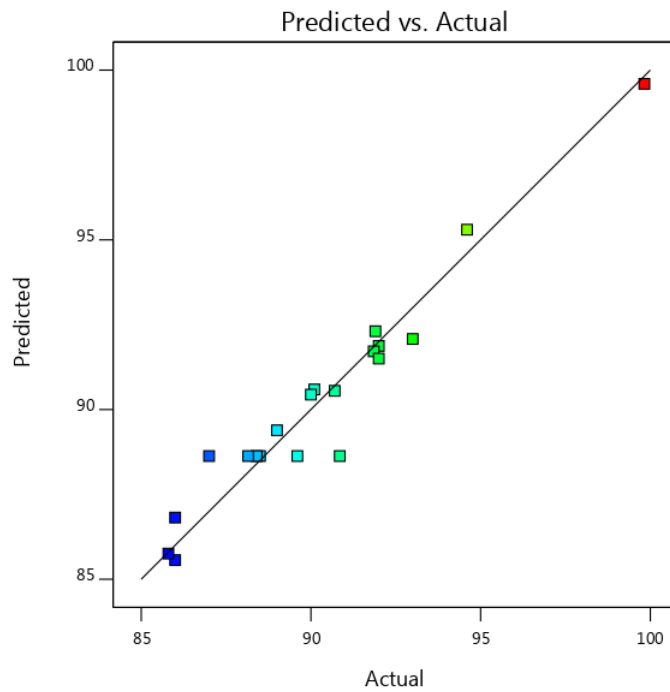




**Figure 5.12: 3 D response surface graph of % Elongation between TRS and TTS**

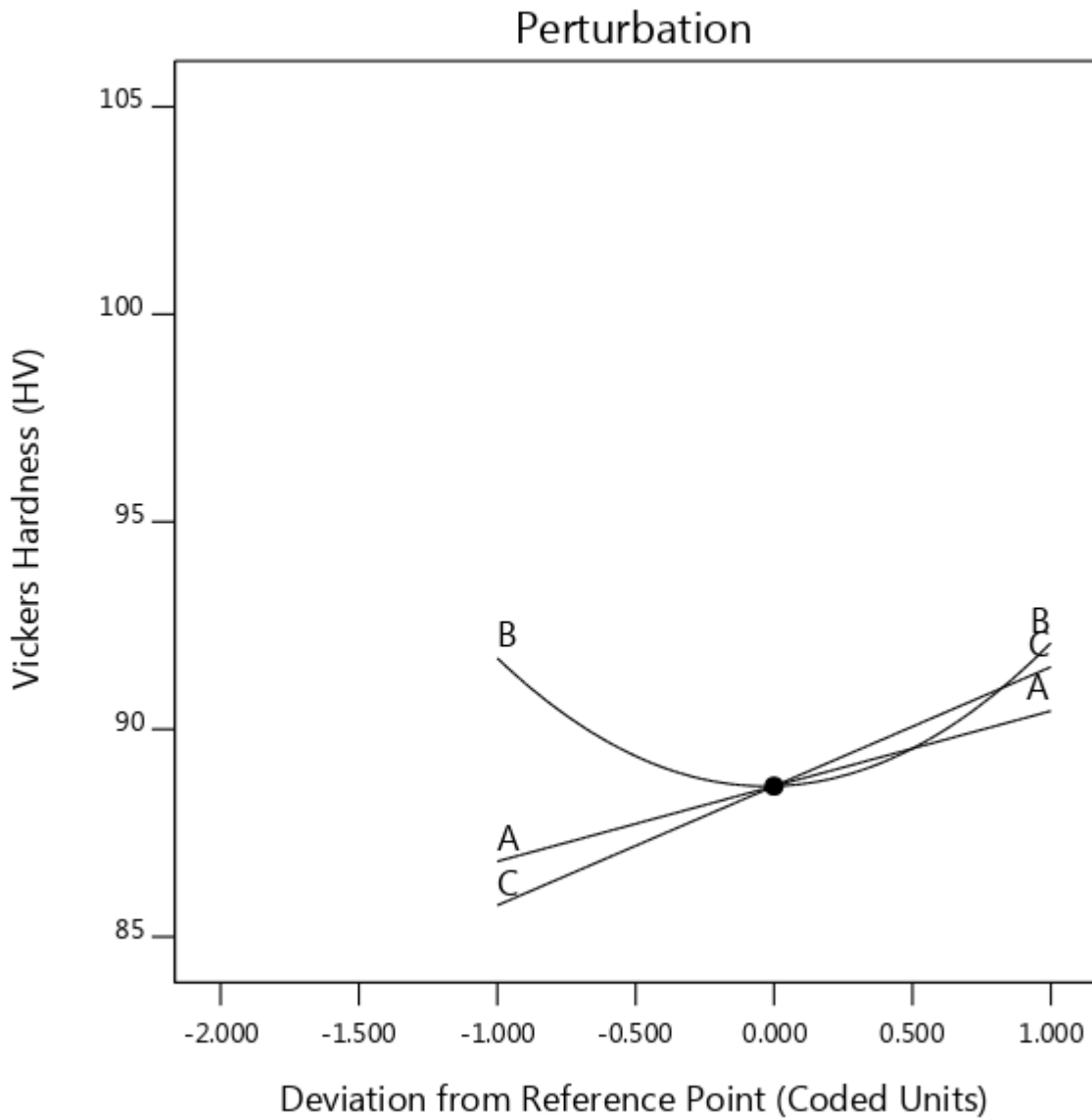
This graph depicts TRS as x1-axis while TTS on the x2-axis, finally % Elongation on y-axis. Response surface geometry is 3-D in nature.

#### 5.1.4 Effect of analysis on Vickers Hardness



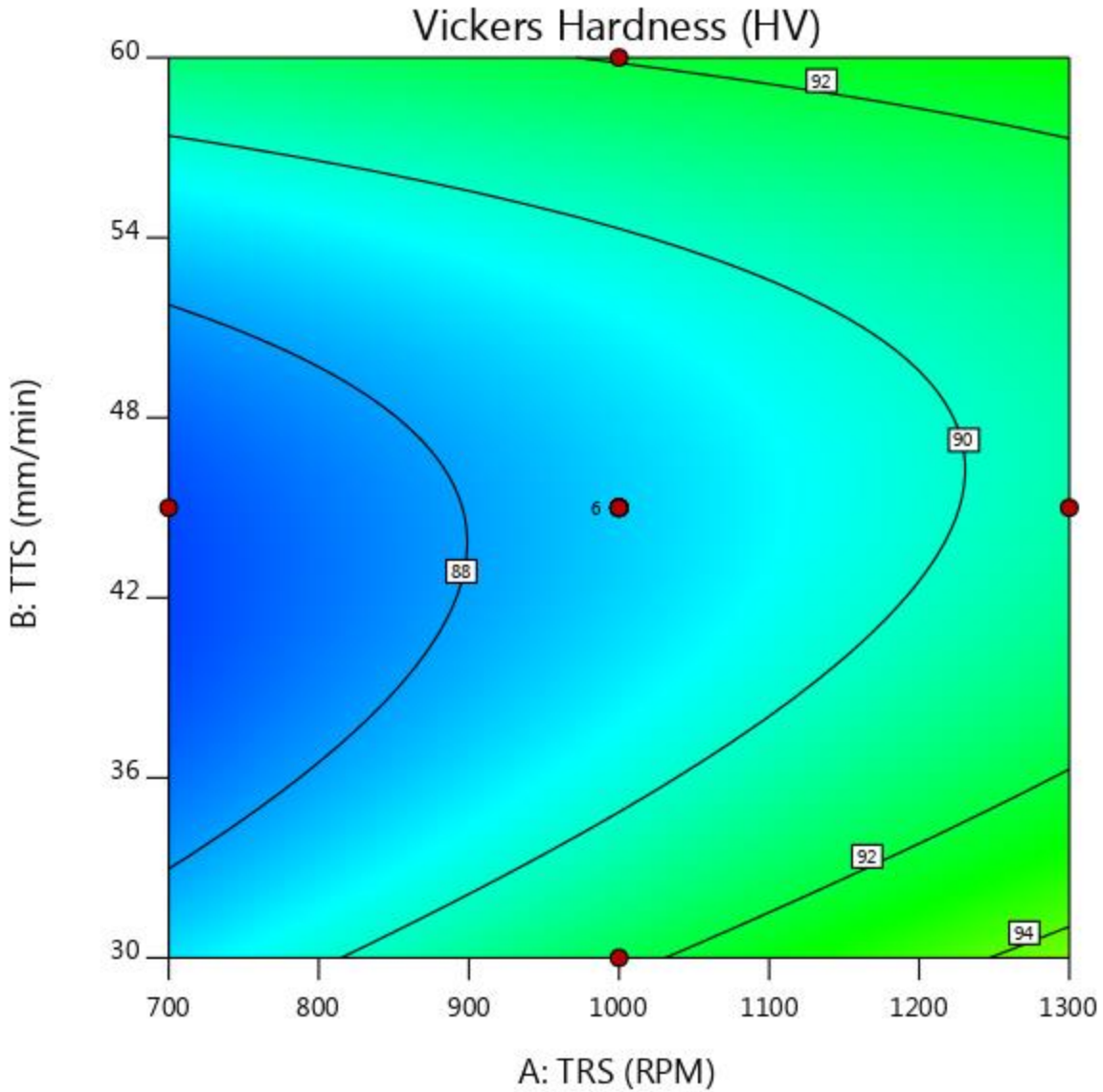
**Figure 5.13: Graph between Predicted vs. Actual points of Vickers Hardness**

The above graph depicts actual data of Vickers Hardness on x-axis while predicted data of Vickers Hardness on the y-axis. Red dots represent highest value of Vickers Hardness while a blue dot represents the least values of Vickers Hardness. From the graph, it is evident that actual data approaches similarity to predicted data.



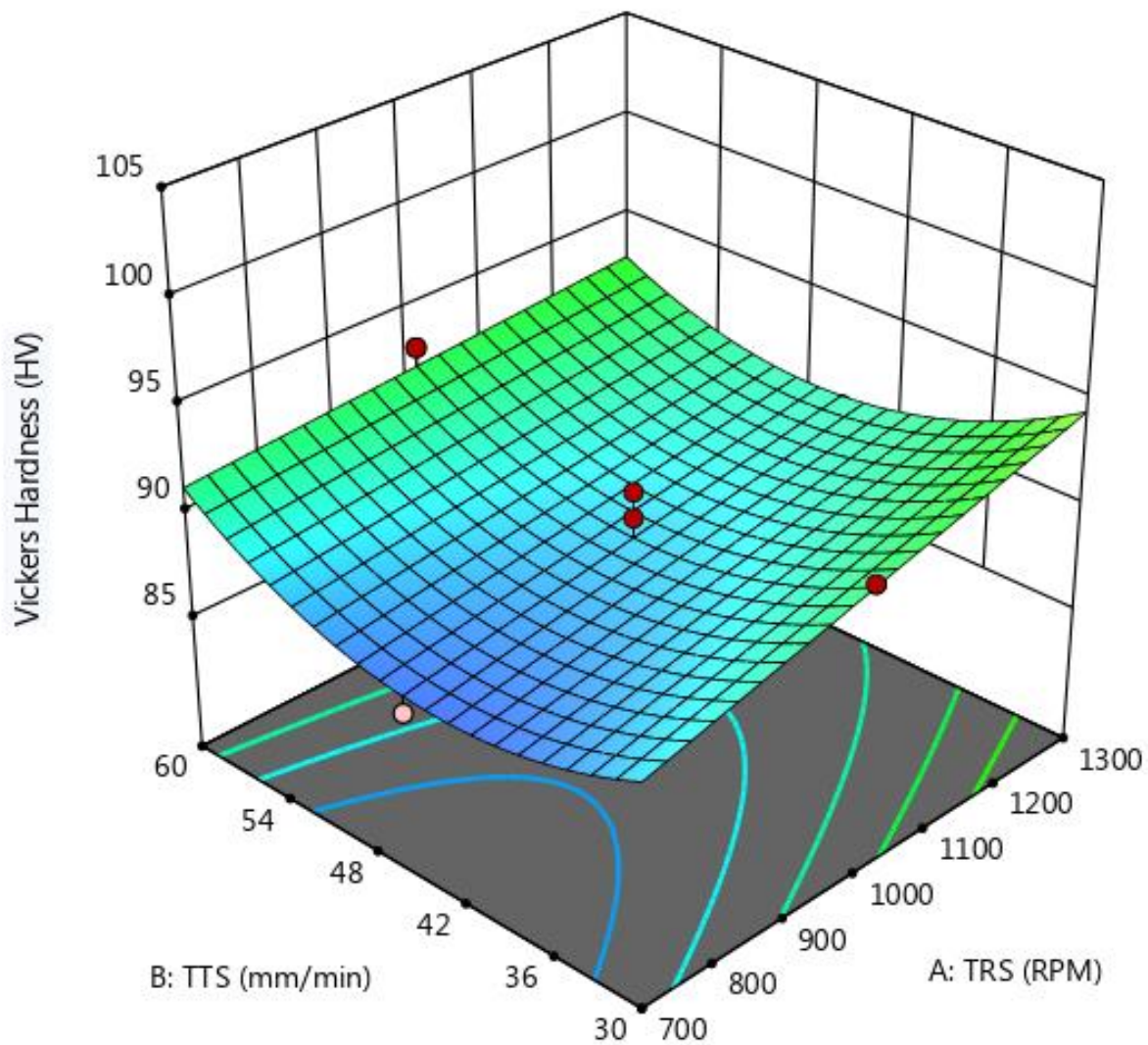
**Figure 5.14: Graph represents the intersection point of Vickers Hardness**

The above graph depicts deviation from reference point on x-axis while Vickers Hardness on the y-axis. This graph is called perturbation curve. In this graph, 3 different coding factors named as A, B and C are intersecting at a point.



**Fig 5.15: Contour plot of Vickers Hardness between TRS and TTS**

This graph depicts, TRS (RPM) on the x-axis while TTS (mm/min) on the y-axis. On this curve, Vickers Hardness point is achieved. Red areas represent maximum value (99.825 HV) of Vickers Hardness while blue areas represent the minimum values of Vickers Hardness (85.8 HV). Contour plots describe the 2-D response surfaces. Contour plots have a crucial part in investigating of the response surfaces. Once created through Software, the profile of surface can be predicted and optimized values are achieved with precision.

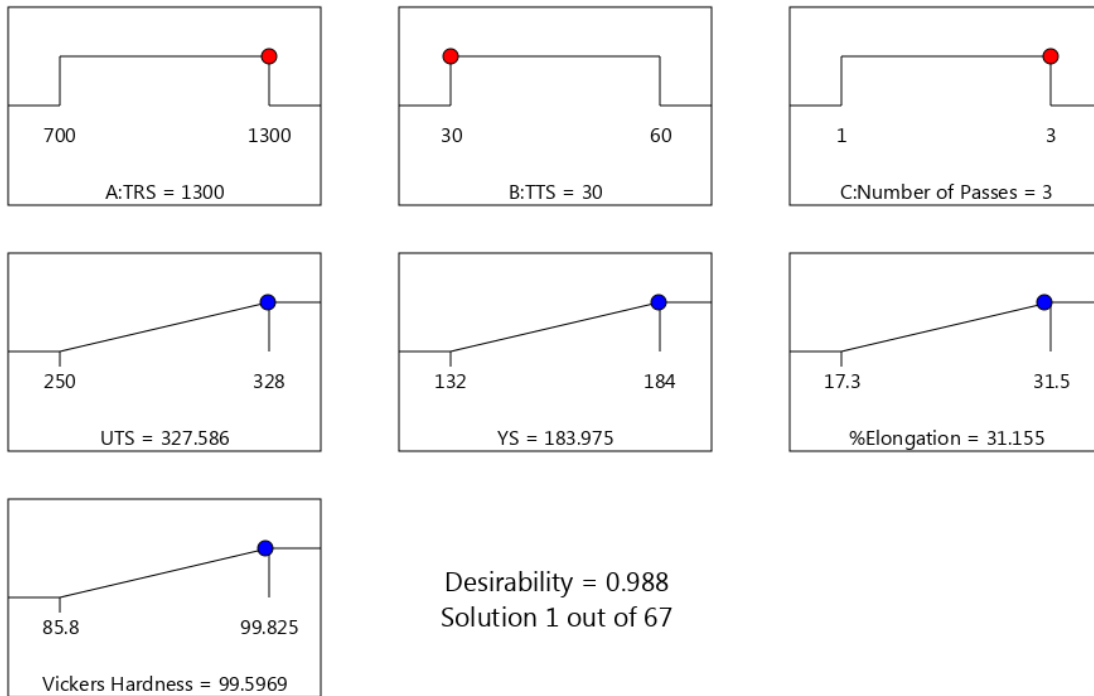


**Figure 5.16: 3 D response surface graph of Vickers Hardness between TRS and TTS**

This graph depicts TRS as x1-axis while TTS on the x2-axis, finally Vickers Hardness on y-axis. Response surface geometry is 3-D in nature.

## 5.2 Optimization of Result

The important step is the optimization of result of the experiment. Optimizations of different response parameter are described following below:



**Figure 5.17: Optimum Result of Factors**

The optimum result has obtained at maximum value of TRS = 1300 MPa , minimum value of TTS = 30 mm/min and number of Passes = 3 unit . The optimum values are for UTS = 327.586 MPa, YS = 183.975 MPa , %Elongation =31.155% and Vickers Hardness= 99 HV with the desirability 98.80 %.

### 5.3 Point Prediction

This Table 5.1 describe the predict the mean of response parameter, Std Dev , 95% CI low for Mean and 95% CI high for Mean on the basis of data points of responses. The point predictions of Responses are following below in the Table 5.1:

**Table 5.1: Predict the mean of Response parameter**

Response	Predicted Mean	Std Dev	95% CI low for Mean	95% CI high for Mean
UTS	327.586	2.94383	322.29	332.883
YS	183.975	2.85555	178.911	189.039
% Elongation	31.155	0.816153	29.7335	32.5765
Vickers Hardness	99.5969	1.00555	97.6681	101.526

## CHAPTER 6

### CONCLUSION AND FUTURE SCOPE OF STUDY

#### 6.1 Conclusions

This dissertation presented the work for the investigation of surface modification of Aluminium Alloy using Friction Stir Processing using Reinforcement of Boron Carbide by adopting Response Surface Methodology for optimisation. Results were generated, on account of which following conclusions can be drawn as:-

- Results presented that UTS has major influential role primarily from Number of Passes having F value of 943.86, followed by TRS with F value of 36.19 and finally TTS having F value of 20.36.
- Results presented that YS has major influential role primarily from Number of Passes having F value of 337.94, followed by TRS with F value of 42.69 and finally TTS having F value of 6.49.
- Results presented that % Elongation has major influential role primarily from Number of Passes having F value of 394.32, followed by TRS with F value of 27.97 and finally TTS having F value of 0.1335.
- Results presented that Vickers Hardness has major influential role primarily from Number of Passes having F value of 81.60, followed by TRS with F value of 32.49 and finally TTS having F value of 0.3294.
- The optimum result has obtained at maximum value of TRS = 1300 MPa , minimum value of TTS = 30 mm/min and number of Passes = 3 unit . The optimum values are for UTS = 327.586 MPa, YS = 183.975 MPa , %Elongation =31.155% and Vickers Hardness= 99 HV with the desirability 98.80 %.
- The interactions between TRS and TTS (A×B), TRS and Number of Passes (A×C) and TTS and Number of Passes (B×C) significantly affect the performance characteristics.

## 6.2 Future Scope of Study

FSP process provides a lot of areas for research and study. Some of the areas are discussed below:

- The AA5083 can be prepared composite with the help of different reinforcements.
- Fabrication of composite can be prepared with different profiles of tool probes.
- Further analysis is required to find out the tool life and residual stress in Friction Stir process.
- The investigation is necessary to assess the impact of ANN in different reinforcement of composite of FSP.

Efforts can be solve the difficulties of problems and made the process efficiently, effectively and productive.

## REFERENCES

- [1] Alaneme, K. K., Bodunrin, M. O., & Awe, A. A. (2018). Microstructure, mechanical and fracture properties of groundnut shell ash and silicon carbide dispersion strengthened aluminium matrix composites. *Journal of King Saud University-Engineering Sciences*, 30(1), 96-103.
- [2] Bodunrin, M. O., Alaneme, K. K., & Chown, L. H. (2015). Aluminium matrix hybrid composites: a review of reinforcement philosophies; mechanical, corrosion and tribological characteristics. *Journal of materials research and technology*, 4(4), 434-445.
- [3] Surappa, M. K. (2003). Aluminium matrix composites: Challenges and opportunities. *Sadhana*, 28(1-2), 319-334.
- [4] Rino, J. J., Chandramohan, D., Sucitharan, K. S., & Jebin, V. D. (2012). An overview on development of aluminium metal matrix composites with hybrid reinforcement. *Int. J. Sci. Res*, 1(3).
- [5] Das, D. K., Mishra, P. C., Singh, S., & Pattanaik, S. (2014). Fabrication and heat treatment of ceramic-reinforced aluminium matrix composites-a review. *International Journal of Mechanical and Materials Engineering*, 9(1), 6.
- [6] Koli, D. K., Agnihotri, G., & Purohit, R. (2015). Advanced aluminium matrix composites: The critical need of automotive and aerospace engineering fields. *Materials Today: Proceedings*, 2(4-5), 3032-3041.
- [7] Ma, Z. Y. (2008). Friction stir processing technology: a review. *Metallurgical and materials Transactions A*, 39(3), 642-658.
- [8] Kurt, A., Uygur, I., & Cete, E. (2011). Surface modification of aluminium by friction stir processing. *Journal of Materials Processing Technology*, 211(3), 313-317.
- [9] Rathee, S., Maheshwari, S., Siddiquee, A. N., & Srivastava, M. (2017). Effect of tool plunge depth on reinforcement particles distribution in surface composite fabrication via friction stir processing. *Defence technology*, 13(2), 86-91.



- [10] Nascimento, F., Santos, T., Vilaça, P., Miranda, R. M., & Quintino, L. (2009). Microstructural modification and ductility enhancement of surfaces modified by FSP in aluminium alloys. *Materials Science and Engineering: A*, 506(1-2), 16-22.
- [11] Mironov, S., Sato, Y. S., & Kokawa, H. (2019). Friction-stir processing. *Nanocrystalline Titanium*, 55–69. doi10.1016b978-0-12-814599-9.00004-3.
- [12] Guru, P. R., Khan, F., Panigrahi, S. K., & Ram, G. J. (2015). Enhancing strength, ductility and machinability of a Al–Si cast alloy by friction stir processing. *Journal of manufacturing processes*, 18, 67-74.
- [13] Sharma, V., Prakash, U., & Kumar, B. M. (2015). Surface composites by friction stir processing: A review. *Journal of Materials Processing Technology*, 224, 117-134.
- [14] Montgomery, D. C. (2017). *Design and analysis of experiments*. John Wiley & sons.
- [15] Vignesh, R. V., & Padmanaban, R. (2018). Influence of friction stir processing parameters on the wear resistance of aluminium alloy AA5083. *Materials Today: Proceedings*, 5(2), 7437-7446.
- [16] Bahrami, A., Pech-Canul, M. I., Gutierrez, C. A., & Soltani, N. (2015). Effect of rice-husk ash on properties of laminated and functionally graded Al/SiC composites by one-step pressureless infiltration. *Journal of Alloys and Compounds*, 644, 256-266.
- [17] Lancaster, L., Lung, M. H., & Sujan, D. (2013, January). Utilization of agro-industrial waste in metal matrix composites: Towards sustainability. In *Proceedings of World Academy of Science, Engineering and Technology* (No. 73, p. 1136). World Academy of Science, Engineering and Technology (WASET).
- [18] Selvam, J. D. R., Smart, D. R., & Dinaharan, I. (2013). Microstructure and some mechanical properties of fly ash particulate reinforced AA6061 aluminum alloy composites prepared by compocasting. *Materials & Design*, 49, 28-34.
- [19] Gopal Krishna, U. B., Sreenivas Rao, K. V., & Vasudeva, B. (2013). Effect of boron carbide reinforcement on aluminium matrix composites. *International Journal of Metallurgical & Materials Science and Engineering (IJMMSE) ISSN*, 41-48.

- [20] <https://www.hudsontoolsteel.com/technical-data/steelH3>, 04/07/2019, 8:25 PM.
- [21] Gopan, V., Sreekumar, P. S., Chandran, J. P., Vijay, W., & Kumar, M. S. (2018). Experimental Investigation on the Effect of Process Parameters on Friction Stir Processing Of Aluminium. *Materials Today: Proceedings*, 5(5), 13674-13681.
- [22] Pol, N., Verma, G., Pandey, R. P., & Shanmugasundaram, T. (2018). Fabrication of AA7005/TiB<sub>2</sub>-B<sub>4</sub>C surface composite by friction stir processing: Evaluation of ballistic behaviour. *Defence Technology*.
- [23] Hosseinzadeh, A., & Yapici, G. G. (2018). High Temperature Characteristics of Al<sub>2</sub>O<sub>3</sub>/SiC Metal Matrix Composite fabricated by Friction Stir Processing. *Materials Science and Engineering: A*.
- [24] Dinaharan, I., & Akinlabi, E. T. (2018). Low cost metal matrix composites based on aluminum, magnesium and copper reinforced with fly ash prepared using friction stir processing. *Composites Communications*, 9, 22-26.
- [25] Zhang, Z. Y., Yang, R., Li, Y., Chen, G., Zhao, Y. T., & Liu, M. P. (2018). Microstructural evolution and mechanical properties of friction stir processed ZrB<sub>2</sub>/6061Al nanocomposites. *Journal of Alloys and Compounds*, 762, 312-318.
- [26] Huang, L., Wang, K., Wang, W., Yuan, J., Qiao, K., Yang, T., ... & Li, T. (2018). Effects of grain size and texture on stress corrosion cracking of friction stir processed AZ80 magnesium alloy. *Engineering Failure Analysis*, 92, 392-404.
- [27] Nadammal, N., Kailas, S. V., Szpunar, J., & Suwas, S. (2018). Development of microstructure and texture during single and multiple pass friction stir processing of a strain hardenable aluminium alloy. *Materials Characterization*, 140, 134-146.
- [28] Huang, G., Hou, W., Li, J., & Shen, Y. (2018). Development of surface composite based on Al-Cu system by friction stir processing: Evaluation of microstructure, formation mechanism and wear behavior. *Surface and Coatings Technology*, 344, 30-42.
- [29] Nene, S. S., Zellner, S., Mondal, B., Komarasamy, M., Mishra, R. S., Brennan, R. E., & Cho, K. C. (2018). Friction stir processing of newly-designed Mg-5Al-3.5 Ca-1Mn (AXM541) alloy: microstructure evolution and mechanical properties. *Materials Science and Engineering: A*.

- [30] Liu, Q., Ma, Q. X., Chen, G. Q., Cao, X., Zhang, S., Pan, J. L., ... & Shi, Q. Y. (2018). Enhanced corrosion resistance of AZ91 magnesium alloy through refinement and homogenization of surface microstructure by friction stir processing. *Corrosion Science*.
- [31] Węglowski, M. S. (2018). Friction stir processing—State of the art. *Archives of civil and Mechanical Engineering*, 18(1), 114-129.
- [32] Padhy, G. K., Wu, C. S., & Gao, S. (2018). Friction stir based welding and processing technologies-processes, parameters, microstructures and applications: A review. *Journal of Materials Science & Technology*, 34(1), 1-38.
- [33] Yadav, D., Bauri, R., & Chawake, N. (2018). Fabrication of Al-Zn solid solution via friction stir processing. *Materials Characterization*, 136, 221-228.
- [34] Zhang, Z. W., Liu, Z. Y., Xiao, B. L., Ni, D. R., & Ma, Z. Y. (2018). High efficiency dispersal and strengthening of graphene reinforced aluminum alloy composites fabricated by powder metallurgy combined with friction stir processing. *Carbon*, 135, 215-223.
- [35] Sudhakar, M., Rao, C. S., & Saheb, K. M. (2018). Production of Surface Composites by Friction Stir Processing-A Review. *Materials Today: Proceedings*, 5(1), 929-935.
- [36] Anshul Chaudhary, Abhishek Kumar Dev, Anshul Goel, Ravi Butola, Ranganath M.S, "The Mechanical Properties of Different alloys in friction stir processing: A Review," *Mater. Today Proc.*, vol. 5, pp. 5553- 5562, 2018.
- [37] Gupta, S. K., Pandey, K. N., & Kumar, R. (2018). Artificial intelligence-based modelling and multi-objective optimization of friction stir welding of dissimilar AA5083-O and AA6063-T6 aluminium alloys. *Proceedings of the Institution of Mechanical Engineers, Part L: Journal of Materials: Design and Applications*, 232(4), 333-342.
- [38] Hussain, G., Ranjbar, M., & Hassanzadeh, S. (2017). Trade-off among mechanical properties and energy consumption in multi-pass friction stir processing of Al7075 alloy employing neural network-based genetic optimization. *Proceedings of the Institution of Mechanical Engineers, Part B: Journal of Engineering Manufacture*, 231(1), 129-139.
- [39] Soleymani, S., Abdollah-Zadeh, A., & Alidokht, S. A. (2012). Microstructural and tribological properties of Al5083 based surface hybrid composite produced by friction stir processing. *Wear*, 278, 41-47.

- [40] Thangarasu, A., Murugan, N., & Dinaharan, I. (2014). Production and wear characterization of AA6082-TiC surface composites by friction stir processing. *Procedia Engineering*, 97, 590-597.
- [41] Rao, A. G., Deshmukh, V. P., Prabhu, N., & Kashyap, B. P. (2016). Enhancing the machinability of hypereutectic Al-30Si alloy by friction stir processing. *Journal of Manufacturing Processes*, 23, 130-134.
- [42] García-Bernal, M. A., Mishra, R. S., Verma, R., & Hernández-Silva, D. (2016). Influence of friction stir processing tool design on microstructure and superplastic behavior of Al-Mg alloys. *Materials Science and Engineering: A*, 670, 9-16.
- [43] Singh, S. K., Immanuel, R. J., Babu, S., Panigrahi, S. K., & Ram, G. J. (2016). Influence of multi-pass friction stir processing on wear behaviour and machinability of an Al-Si hypoeutectic A356 alloy. *Journal of Materials Processing Technology*, 236, 252-262.
- [44] Meenia, S., Khan, F., Babu, S., Immanuel, R. J., Panigrahi, S. K., & Ram, G. J. (2016). Particle refinement and fine-grain formation leading to enhanced mechanical behaviour in a hypo-eutectic Al-Si alloy subjected to multi-pass friction stir processing. *Materials Characterization*, 113, 134-143.
- [45] Joyson Abraham, S., Chandra Rao Madane, S., Dinaharan, I., & John Baruch, L. (2016). Development of quartz particulate reinforced AA6063 aluminum matrix composites via friction stir processing. *Journal of Asian Ceramic Societies*, 4(4), 381-389.
- [46] Dinaharan, I., Murugan, N., & Thangarasu, A. (2016). Development of empirical relationships for prediction of mechanical and wear properties of AA6082 aluminum matrix composites produced using friction stir processing. *Engineering science and technology, an international journal*, 19(3), 1132-1144.
- [47] Dinaharan, I., Sathiskumar, R., & Murugan, N. (2016). Effect of ceramic particulate type on microstructure and properties of copper matrix composites synthesized by friction stir processing. *Journal of Materials Research and Technology*, 5(4), 302-316.
- [48] KIRAN, G. S., Krishna, K. H., Sameer, S. K., Bhargavi, M., Kumar, B. S., Rao, G. M., ... & Sunil, B. R. (2017). Machining characteristics of fine grained AZ91 Mg alloy processed by friction stir processing. *Transactions of Nonferrous Metals Society of China*, 27(4), 804-811.

- [49] Yuvaraj, N., & Aravindan, S. (2017). Comparison studies on mechanical and wear behavior of fabricated aluminum surface nano composites by fusion and solid state processing. *Surface and Coatings Technology*, 309, 309-319.
- [50] Węglowski, M. S. (2018). Friction stir processing—State of the art. *Archives of civil and mechanical engineering*, 18(1), 114-129.
- [51] Lashgari, H. R., Kong, C., Asnavandi, M., & Zangeneh, S. (2018). The effect of friction stir processing (FSP) on the microstructure, nanomechanical and corrosion properties of low carbon CoCr28Mo5 alloy. *Surface and Coatings Technology*, 354, 390-404.
- [52] Kurkute, V., & Chavan, S. T. (2018). Modeling and Optimization of surface roughness and microhardness for roller burnishing process using response surface methodology for Aluminum 63400 alloy. *Procedia Manufacturing*, 20, 542-547.
- [53] Zhao, H., Pan, Q., Qin, Q., Wu, Y., & Su, X. (2019). Effect of the processing parameters of friction stir processing on the microstructure and mechanical properties of 6063 aluminum alloy. *Materials Science and Engineering: A*, 751, 70-79.
- [54] Arulmoni, V. J., & Mishra, R. S. (2014). Friction Stir Processing of Aluminium alloys for Defense Applications. *International Journal of Advance Research and Innovation*, 2(2), 337-341.
- [55] Sharifitabar, M., Sarani, A., Khorshahian, S., & Afarani, M. S. (2011). Fabrication of 5052Al/Al<sub>2</sub>O<sub>3</sub> nanoceramic particle reinforced composite via friction stir processing route. *Materials & Design*, 32(8-9), 4164-4172.
- [56] Khan, F., Karthik, G. M., Panigrahi, S. K., & Ram, G. J. (2019). Friction stir processing of QE22 magnesium alloy to achieve ultrafine-grained microstructure with enhanced room temperature ductility and texture weakening. *Materials Characterization*, 147, 365-378.
- [57] Maamoun, A. H., Xue, Y. F., Elbestawi, M. A., & Veldhuis, S. C. (2018). Effect of SLM process parameters on the quality of Al alloy parts; part II: microstructure and mechanical properties.
- [58] Rubino, F., Scherillo, F., Franchitti, S., Squillace, A., Astarita, A., & Carlone, P. (2019). Microstructure and surface analysis of friction stir processed Ti-6Al-4V plates manufactured by electron beam melting. *Journal of Manufacturing Processes*, 37, 392-401.
- [59] Heidarpour, A., Mazaheri, Y., Roknian, M., & Ghasemi, S. (2019). Development of Cu-TiO<sub>2</sub> surface nanocomposite by friction stir processing: Effect of pass number on microstructure,

mechanical properties, tribological and corrosion behavior. *Journal of Alloys and Compounds*, 783, 886-897.

[60] Jin, Y., Wang, K., Wang, W., Peng, P., Zhou, S., Huang, L., ... & Cai, J. (2019). Microstructure and mechanical properties of AE42 rare earth-containing magnesium alloy prepared by friction stir processing. *Materials Characterization*, 150, 52-61.

[61] Tang, J., Shen, Y., & Li, J. (2019). Influences of friction stir processing parameters on microstructure and mechanical properties of SiC/Al composites fabricated by multi-pin tool. *Journal of Manufacturing Processes*, 38, 279-289.

[62] Fotoohi, H., Lotfi, B., Sadeghian, Z., & Byeon, J. W. (2019). Microstructural characterization and properties of in situ Al-Al<sub>3</sub>Ni/TiC hybrid composite fabricated by friction stir processing using reactive powder. *Materials Characterization*, 149, 124-132.

[63] Khorrami, M. S., Saito, N., & Miyashita, Y. (2019). Texture and strain-induced abnormal grain growth in cryogenic friction stir processing of severely deformed aluminum alloy. *Materials Characterization*, 151, 378-389.

[64] Xu, N., Song, Q., & Bao, Y. (2019). {10–12} twinning assisted microstructure and mechanical properties modification of high-force friction stir processed AZ31B Mg alloy. *Materials Science and Engineering: A*, 745, 400-403.

[65] Sharma, A., Sharma, V. M., Sahoo, B., Pal, S. K., & Paul, J. (2019). Effect of multiple micro channel reinforcement filling strategy on Al6061-graphene nanocomposite fabricated through friction stir processing. *Journal of Manufacturing Processes*, 37, 53-70.

[66] Huang, G. Q., Yan, Y. F., Wu, J., Shen, Y. F., & Gerlich, A. P. (2019). Microstructure and mechanical properties of fine-grained aluminum matrix composite reinforced with nitinol shape memory alloy particulates produced by underwater friction stir processing. *Journal of Alloys and Compounds*, 786, 257-271.

[67] Kumar, S., Singh, S. K., Kumar, J., & Murtaza, Q. (2018). Synthesis and Characterization of Al-alloy by Mechanical alloying. *Materials Today: Proceedings*, 5(2), 3237-3242.

# the aluminium composite

---

## ORIGINALITY REPORT

---

10%

SIMILARITY INDEX

6%

INTERNET SOURCES

7%

PUBLICATIONS

8%

STUDENT PAPERS

---

## PRIMARY SOURCES

---

- |   |  |     |
|---|--|-----|
| 1 | Submitted to Maulana Azad National Institute of Technology Bhopal<br>Student Paper   | 2%  |
| 2 | R. Vaira Vignesh, R. Padmanaban. "Influence of friction stir processing parameters on the wear resistance of aluminium alloy AA5083",<br>Materials Today: Proceedings, 2018<br>Publication   | 1%  |
| 3 | Submitted to Caledonian College of Engineering<br>Student Paper  | 1%  |
| 4 | <a href="http://krishikosh.egranth.ac.in">krishikosh.egranth.ac.in</a><br>Internet Source  | 1%  |
| 5 | <a href="http://www.chemijournal.com">www.chemijournal.com</a><br>Internet Source  | 1%  |
| 6 | BERBER, Adnan. "Mathematical Model for Fuel Flow Performance of Diesel Engine", Selçuk Üniversitesi Alaeddin Keykubat Kampüsü Teknik Eğitim Fakültesi Selçuklu / Konya, 2016.<br>Publication | <1% |
-

- |    |  |     |
|----|--|-----|
| 7  | Submitted to Nelson Mandela Metropolitan University<br>Student Paper   | <1% |
| 8  | Submitted to Universiti Malaysia Kelantan<br>Student Paper   | <1% |
| 9  | Submitted to Jawaharlal Nehru Technological University<br>Student Paper  | <1% |
| 10 | B. Rajeswari, K. S. Amirthagadeswaran. "Study of machinability and parametric optimization of end milling on aluminium hybrid composites using multi-objective genetic algorithm", Journal of the Brazilian Society of Mechanical Sciences and Engineering, 2018<br>Publication              | <1% |
| 11 | N Fatchurrohman, N Farhana, C D Marini. "Investigation on the effect of Friction Stir Processing Parameters on Micro-structure and Micro-hardness of Rice Husk Ash reinforced Al6061 Metal Matrix Composites", IOP Conference Series: Materials Science and Engineering, 2018<br>Publication | <1% |
| 12 | <a href="http://www.inderscience.com">www.inderscience.com</a><br>Internet Source  | <1% |
| 13 | <a href="http://etheses.whiterose.ac.uk">etheses.whiterose.ac.uk</a>   |     |



<1%

14

Submitted to Durban University of Technology

Student Paper

<1%

15

[www.ijsrp.org](http://www.ijsrp.org)

Internet Source

<1%

16

Submitted to Middle East Technical University

Student Paper

<1%

17

V Gunaraj, N Murugan. "Application of response surface methodology for predicting weld bead quality in submerged arc welding of pipes", Journal of Materials Processing Technology, 1999

Publication

<1%

18

[ujcontent.uj.ac.za](http://ujcontent.uj.ac.za)

Internet Source

<1%

19

Submitted to National Institute Of Technology, Tiruchirappalli

Student Paper

<1%

20

[springerplus.springeropen.com](http://springerplus.springeropen.com)

Internet Source

<1%

21

Hrishikesh Das, Mounarik Mondal, Sung-Tae Hong, Doo-Man Chun, Heung Nam Han.

"Joining and fabrication of metal matrix composites by friction stir welding/processing",

<1%

# International Journal of Precision Engineering and Manufacturing-Green Technology, 2018

Publication

22

Marek Stanisław Węglowski. "Friction stir processing – State of the art", Archives of Civil and Mechanical Engineering, 2018

Publication

<1%

23

Submitted to Charotar University of Science And Technology

Student Paper

<1%

24

Submitted to Delhi Technological University

Student Paper

<1%

25

Submitted to British University in Egypt

Student Paper

<1%

26

Submitted to Pacific University

Student Paper

<1%

27

Mahmoud, T.S.. "Surface modification of A390 hypereutectic Al–Si cast alloys using friction stir processing", Surface and Coatings Technology, 2013.

Publication

<1%

28

[www.tandfonline.com](http://www.tandfonline.com)

Internet Source

<1%

29

Submitted to University of Sheffield

Student Paper

<1%

30

R Vaira Vignesh, R Padmanaban, M Govindaraju. "Investigations on the surface topography, corrosion behavior, and biocompatibility of friction stir processed magnesium alloy AZ91D", Surface Topography: Metrology and Properties, 2019

Publication

&lt;1%

31

tjprc.org  
Internet Source

&lt;1%

32

Gyander Ghangas, Sandeep Singhal. "Effect of tool pin profile and dimensions on mechanical properties and microstructure of friction stir welded armor alloy", Materials Research Express, 2018

Publication

&lt;1%

33

Nitinkumar Pol, Gaurav Verma, R.P. Pandey, T. Shanmugasundaram. "Fabrication of AA7005/TiB<sub>2</sub>-B<sub>4</sub>C surface composite by friction stir processing: Evaluation of ballistic behaviour", Defence Technology, 2019

Publication

&lt;1%

34

www.ijeat.org  
Internet Source

&lt;1%

35

Nalin Somani, Y K Tyagi, Parveen Kumar, Vineet Srivastava, Hiralal Bhowmick. "Enhanced tribological properties of SiC reinforced copper

&lt;1%

metal matrix composites", Materials Research Express, 2018

Publication

36

[corrosionjournal.org.pinnacle.allenpress.com](http://corrosionjournal.org.pinnacle.allenpress.com)

Internet Source

<1%

37

[doaj.org](http://doaj.org)

Internet Source

<1%

38

Submitted to Higher Education Commission  
Pakistan

Student Paper

<1%

39

Singh, Satnam, Manish Garg, and N. K. Batra.  
"Analysis of Dry Sliding Behavior of  
Al<sub>2</sub>O<sub>3</sub>/B<sub>4</sub>C/Gr Aluminum Alloy Metal Matrix  
Hybrid Composite Using Taguchi Methodology",  
Tribology Transactions, 2015.

Publication

<1%

40

R. Soundararajan, A. Ramesh, S. Sivasankaran,  
M. Vignesh. "Modeling and Analysis of  
Mechanical Properties of Aluminium Alloy  
(A413) Reinforced with Boron Carbide (B<sub>4</sub>C)  
Processed Through Squeeze Casting Process  
Using Artificial Neural Network Model and  
Statistical Technique", Materials Today:  
Proceedings, 2017

Publication

<1%

41

[www.ijapjournal.com](http://www.ijapjournal.com)

Internet Source

<1%

---

42

# Submitted to University of Macau

Student Paper

<1%

---

---

Exclude quotes      On

Exclude matches      < 10 words

Exclude bibliography      On